



BRNO UNIVERSITY OF TECHNOLOGY

VYSOKÉ UČENÍ TECHNICKÉ V BRNĚ

FACULTY OF ELECTRICAL ENGINEERING AND COMMUNICATION

FAKULTA ELEKTROTECHNIKY
A KOMUNIKAČNÍCH TECHNOLOGIÍ

DEPARTMENT OF RADIO ELECTRONICS

ÚSTAV RADIOELEKTRONIKY

COMPACT ANTENNA SYSTEM FOR SATELLITE SIGNALS RECEPTION IN UHF BAND

KOMPAKTNÍ ANTÉNNÍ SYSTÉM PRO PŘÍJEM DRUŽICOVÝCH SIGNÁLŮ V UHF PÁSMU

MASTER'S THESIS

DIPLOMOVÁ PRÁCE

AUTHOR

AUTOR PRÁCE

Bc. Vladimír Lukáč

SUPERVISOR

VEDOUCÍ PRÁCE

Ing. Tomáš Urbanec, Ph.D.

BRNO 2024

Master's Thesis

Master's study program **Electronics and Communication Technologies**

Department of Radio Electronics

Student: Bc. Vladimír Lukáč

ID: 221340

Year of

2

Academic year: 2023/24

study:

TITLE OF THESIS:

Compact Antenna System for Satellite Signals Reception in UHF Band

INSTRUCTION:

MP(K)C-M2E: Perform a statistical evaluation of the position of the satellite in low orbit relative to the ground station. Determine the potential benefit of coverage reduction and sectorization. Create a compact antenna model in HFSS with the reception of two linear polarizations perpendicular to each other.

MP(K)C-MSE: Optimize the antenna model with regard to meeting the maximum reception time of the selected satellite. Design the feed network for the antenna, design the mechanical structure of the antenna suitable for implementation, and implement the antenna. Verify its parameters and possibly suggest potential improvements to the structure.

RECOMMENDED LITERATURE:

[1] CARR, Joseph. Practical Antenna Handbook. Fourth edition. McGraw-Hill: TAB Electronics, [2001]. ISBN 978-0071374354

[2] BALANIS, Constantine A. Antenna theory: analysis and design. Fourth edition. Hoboken: Wiley, [2016]. ISBN 978-1-118-64206-1.

Date of project

specification: 16.2.2024

Deadline for

submission: 20.5.2024

Supervisor: Ing. Tomáš Urbanec, Ph.D.

doc. Ing. Lucie Hudcová, Ph.D.

Chair of study program board

WARNING:

The author of the Master's Thesis claims that by creating this thesis he/she did not infringe the rights of third persons and the personal and/or property rights of third persons were not subjected to derogatory treatment. The author is fully aware of the legal consequences of an infringement of provisions as per Section 11 and following of Act No 121/2000 Coll. on copyright and rights related to copyright and on amendments to some other laws (the Copyright Act) in the wording of subsequent directives including the possible criminal consequences as resulting from provisions of Part 2, Chapter VI, Article 4 of Criminal Code 40/2009 Coll.

Abstract

This thesis describes the design of an antenna array for the reception of satellite signals in the UHF band. In this thesis, methods of obtaining information about the satellite and their statistical evaluation are presented. Based on the information obtained, the selected antenna is designed. The designed single antenna is simulated in the HFSS Ansys program. The simulations take into account the maximum gain, the reflection coefficient and the bandwidth of the antenna. Base model and results are later used for antenna array. With the same methods, the antenna array is tested in the simulator as the single antenna. Based on the simulations, the single antenna is physically made and measured. The results obtained from the single antenna serve as basis for creating the antenna array.

Keywords

satellite, elevation, azimuth, gain, square patch antenna, coaxial feed, reflection factor S_{11} , radiation pattern, antenna array

Abstrakt

Táto práca popisuje návrh anténnej rady pre príjem družicových signálov v UHF pásme. V práci sú uvedené metódy získania informácií o družici a ich štatistické vyhodnotenie. Na základe získaných informácií sa navrhne vybraná antenna. Navrnutá jednoprvková anténa je simulovaná v programu HFSS Ansys. V simulácií sa berie ohľad na maximálny zisk, činiteľ odrazu a šírka pásma antény. Základný model a výsledky sú potom použité pre tvorbu anténneho poľa. Rovnakým spôsobom, anténne pole je testované v simulátore ako jednoprvková antenna. Na základe simulácií, jednoprvková anténa je fyzicky vyrobené a odmerané. Získané výsledky z jednoprvkovej antény poslúžia ako základ pri vytváraní anténneho poľa.

Klíčov^á slova

družica, elevácia, azimuth, zisk, štvorcová fličková anténa, koaxiálne napájanie, činiteľ odrazu S_{11} , graf polárneho žiarenia, anténne pole

Rozšírený abstrakt

Táto práca, menom Kompaktný anténny systém pre príjem družicových signálov v UHF pásme, pozostáva zo štatistickej časti, návrhu a výpočtu parametrov pre jednu anténu, modelovania a simulácie jednej antény v simulátore HFSS Ansys, návrh, modelovanie a simulácia anténneho poľa a ako posledné fyzická realizácia anténneho poľa s vhodne navrhnutou konštrukciou. Štatistická časť práce sa zaoberá získavaním a spracovaním údajov zo satelitu. Najdôležitejšími údajmi pre vhodný návrh anténneho poľa sú uhly azimutu a elevácie pre zvolené miesto fyzického merania (v tomto prípade Brno). Ďalšie dôležité parametre sú dosah antény (vzdialenosť) k satelitu a perióda satelitu okolo Zeme. Vyhodnotené údaje pre zvolené miesto fyzického merania budú porovnané s miestom, ktoré je umiestnené úplne na severu. Po štatistickom vyhodnotení je možné anténu navrhnuť. V tomto prípade sa navrhne dizajn jednej antény, ktorá bude slúžiť ako vzor pre anténne pole. Niektoré parametre antény, ako napríklad rezonančná frekvencia, šírka pásma a samotný typ antény, určuje vedúci práce. V niektorých prípadoch je potrebné si niektoré parametre určiť, ako napríklad rozmer antény. Pri návrhu jednej antény sa ako prvé zvolí vhodný dielektrický substrát, potom sa vypočítajú parametre antény, ako napríklad fyzický rozmer antény a nakoniec sa navrhne napájanie antény, ktoré bude budiť anténu. Po dokončení návrhu jednej antény sa anténa namodeluje a odsimuluje. Anténa bude modelovaná a simulovaná v programe HFSS Ansys. Dôležitými údajmi pri simulácii jednej antény sú graf činiteľa odrazu na vstupe antény a graf vyžarovania antény. Pri pohľade na graf činiteľa odrazu na vstupe sa dokáže určiť simulovaná rezonančná frekvencia antény, hodnota samotného činiteľa odrazu na vstupe a šírka pásma antény. Vyžarovací diagram antény hovorí o smeru žiarenia, o celkovom zisku a útlmu antény. Dôležitými bodmi vyžarovania antény sú smer, veľkosť hlavného laloku a celkový zisk hlavného laloku. Ďalšie dôležité body u vyžarovania antény sú vedľajšie laloky a spätný lalok. Tieto laloky musia ostať tlmené. V opačnom prípade môže dôjsť k stratám. Posledným bodom simulácie jednej antény je overenie funkčnosti a stability navrhnutého modelu. Použitou metódou overenia funkčnosti modelu je napríklad pridanie druhého napájacieho bodu (symetrického), v tomto prípade horizontálne a vertikálne. Hlavným cieľom je overiť, či sa činiteľ odrazu na vstupe bude líšiť od pôvodného. Pri drastickom znížení hodnoty činiteľa odrazu alebo posunu rezonančnej veľkosti antény je možné považovať model za nestabilný. V takomto prípade je potrebné model prerobiť. Taktiež sa overí stabilita modelu antény pri vyžarovaní do všetkých svetových strán. Rozdiel je v tom, že okolo zvolenej antény budú postavené len 3 dodatočné reflektory namiesto plných modelov, kde každý z reflektorov reprezentuje svetovú stranu. Podobne ako v prípade symetrického napájania sa bude overovať rezonančná frekvencia modelu antény a veľkosť činiteľa odrazu na vstupe. K tomuto sa pridá aj overenie celkového zisku antény vykreslením grafu vyžarovania antény. V tomto prípade sa pozoruje zmena zisku a tvar grafu vyžarovania. Ak je pokles zisku príliš veľký alebo tvar grafu vyžarovania

príliš odlišný od originálu, tak je potrebné anténu prerobiť alebo navrhnuť kompletne nový model. Ak model jednej antény funguje ako má, tak sa môže tento model použiť pri tvorbe anténneho poľa. Anténne pole pozostáva z 2 alebo viacerých druhov tej samej antény [23]. Keďže cieľom tejto práce je navrhnuť kompaktný anténny systém, je potrebné dbať na výsledné rozmery antény. Na rozdiel od jednej antény, na anténne pole je možné aplikovať metódy, ktoré dokážu ovplyvniť výsledok, napríklad celkový zisk, pozitívne alebo aj negatívne. Tieto metódy sa aplikujú pre čo najoptimálnejší dizajn anténneho poľa. Potom sa pokračuje podobným spôsobom ako pri dizajne jednej antény. Zistí sa hodnota činiteľov odrazu a skontroluje sa šírka pásma anténneho poľa spolu s rezonančnou frekvenciou, prípadne sa anténa naladí na potrebnú rezonančnú frekvenciu. Následne sa vykreslí vyžarovací graf a skontroluje sa, či sú vedľajšie laloky a spätný lalok utlmené. Zisk antény (hlavný lalok) musí byť väčší, ako zisk jednej antény, hlavný dôvod pre anténne pole je práve čo najväčší dosiahnuteľný zisk. Avšak je potrebné dbať na rozmery výslednej antény. Dosiahnuté výsledky sa následne porovnávajú s iným modelom, ktorý by potenciálne mohol fungovať. Iný model môže byť napríklad úplne iný typ antény alebo rovnaký typ antény s rôznym počtom prvkov v poli. Anténne pole sa následne overí rovnakými spôsobmi ako pri návrhu jednej antény. Samozrejme, pre dosiahnuté výsledky platí taktiež to samé. Ak sú výsledky príliš odlišné od originálu, tak je potrebné návrh prerobiť a skontrolovať znovu. Po overení výsledkov simulácie sa vyrobí reálny, fyzický model jednej antény a anténneho poľa, prípadne sa použije alternatívny spôsob pre anténne pole kvôli veľkým rozmerom a komplexnosti. Jedná anténa sa vyrába z dôvodu overenia funkčnosti návrhu a správnosť výsledkov, prípadne k vyhľadaniu potenciálnych väd na anténne a vysvetliť ich, ako napríklad nesprávne rozmery žiariča, skutočné parametre dielektrika (napr. relatívna permitivita), zle vyvrtaná diera pre napájanie, a podobne. Po overení funkčnosti fyzického modelu jednej antény sa vyrobí anténne pole s aplikovanými zmenami (ak nejaké sú), ktoré sa zistili pri testovaní jednej antény.

Bibliographic citation

LUKÁČ, Vladimír. *Kompaktní anténní systém pro příjem družicových signálů v UHF pásmu* [online]. Brno, 2024 [cit. 2024-05-20]. Dostupné z: <https://www.vut.cz/studenti/zav-prace/detail/159067>. Diplomová práce. Vysoké učení technické v Brně, Fakulta elektrotechniky a komunikačních technologií, Ústav radioelektroniky. Vedoucí práce Tomáš Urbanec.

Author's Declaration

Author:	Vladimír Lukáč
Author's ID:	221340
Paper type:	Master's Thesis
Academic year:	2023/24
Topic:	Compact Antenna System for Satellite Signals Reception in UHF Band

I declare that I have written this paper independently, under the guidance of the advisor and using exclusively the technical references and other sources of information cited in the project and listed in the comprehensive bibliography at the end of the project.

As the author, I furthermore declare that, with respect to the creation of this paper, I have not infringed any copyright or violated anyone's personal and/or ownership rights. In this context, I am fully aware of the consequences of breaking Regulation S 11 of the Copyright Act No. 121/2000 Coll. of the Czech Republic, as amended, and of any breach of rights related to intellectual property or introduced within amendments to relevant Acts such as the Intellectual Property Act or the Criminal Code, Act No. 40/2009 Coll., Section 2, Head VI, Part 4.

Brno, May 19, 2024

author's signature

Acknowledgement

I would like to thank my supervisor Ing. Tomáš Urbanec, Ph.D. for the possibility of project elaboration under his leadership, for his valuable and professional advice, willingness, and helpful approach during work processing.

I'm also grateful to doc. Ing. Jaroslav Lačík, Ph.D. for verifying the measured data for me and explaining them.

Brno, May 19, 2024

Author's signature

Contents

1. STATISTIC	11
1.1 DATA ACQUISITION OF SATELLITE POSITION.....	11
1.2 DATA EVALUATION	12
1.2.1 <i>Elevation</i>	13
1.2.2 <i>Azimuth</i>	15
1.2.3 <i>Gain</i>	16
2. ANTENNA DESIGN.....	19
2.1 DIELECTRIC SUBSTRATE.....	19
2.1.1 <i>FR4</i>	19
2.1.2 <i>Nylatron</i>	19
2.1.3 <i>Ertalon 6</i>	20
2.2 DIMENSIONS OF SQUARE PATCH	20
2.3 COAXIAL FEED AND IMPEDANCE ON THE EDGE.....	22
3. SINGLE ANTENNA	25
3.1 ANTENNA MODELING	25
3.1.1 <i>Impedance change</i>	26
3.2 EXPERIMENTING WITH ANTENNA DIMENSIONS	26
3.2.1 <i>Dependence of the height on bandwidth and gain</i>	26
3.2.2 <i>Dependence of the ground plane on antenna gain</i>	28
3.3 REFLECTION COEFFICIENT.....	28
3.4 RADIATION PATTERN.....	29
3.5 VERIFICATION OF SINGLE ANTENNA	32
4. ANTENNA ARRAY.....	35
4.1 ARRAY DESIGN.....	35
4.1.1 <i>Feeding methods</i>	37
4.1.2 <i>Miscellaneous changes</i>	38
4.2 REFLECTION COEFFICIENT.....	39
4.3 RADIATION PATTERN.....	41
4.4 COMPARISON BETWEEN TWO AND THREE-ELEMENT ARRAY.....	43
4.5 VERIFICATION OF THE ANTENNA ARRAY	46
5. ANTENNA BUILDING AND TESTING.....	49
5.1 BUILDING AND TESTING THE SINGLE ANTENNA	49
5.1.1 <i>Troubleshooting</i>	51
5.1.2 <i>Redesigning, Rebuilding and testing</i>	52
5.2 VERIFICATION THROUGH .SAT FILE	53
6. CONCLUSION.....	56

FIGURES

Fig. 1.1: SatPC32 Interface	11
Fig. 1.2: Output data from WinListen program	12
Fig. 1.3: The angle of elevation between the antenna and satellite	13
Fig. 1.4: Histogram of elevation for Brno.....	14
Fig. 1.5: Histogram of elevation for Longyearbyen.....	14
Fig. 1.6: The angle of azimuth of the antenna and the satellite.....	15
Fig. 1.7: Histogram of azimuth for Brno	16
Fig. 1.8: Histogram of azimuth for Longyearbyen	16
Fig. 1.9: Potential gain for Brno and Longyearbyen.....	17
Fig. 1.10: Ideal radiation pattern of the antenna (vertical section - elevation).....	18
Fig. 2.1: Square Patch antenna with coaxial feeding	20
Fig. 2.2: Coaxial feed in 3 different positions (TOP side)	23
Fig. 3.1: Modeled square patch antenna in HFSS Ansys	25
Fig. 3.2: Dependence of the bandwidth on the substrate height.....	27
Fig. 3.3: Dependence of the total gain on the substrate height	27
Fig. 3.4: Dependence of the gain on the ground length of the antenna	28
Fig. 3.5: Reflection coefficient s_{11} with different position of coaxial feed	29
Fig. 3.6: Reflection coefficient s_{11} and bandwidth of the tuned antenna	29
Fig. 3.7: Square patch antenna with expanded ground plane	30
Fig. 3.8: Radiation pattern of the antenna – E-plane (GND and patch are same)	30
Fig. 3.9: Radiation pattern of the square patch antenna – E-plane.....	31
Fig. 3.10: 3D gain plot of the square patch antenna.....	31
Fig. 3.11: Square patch antenna with 2 coaxial probes	32
Fig. 3.12: Reflection coefficients of the antenna – functionality test.....	32
Fig. 3.13: Model of the antenna for main directions test	33
Fig. 3.14: Reflection coefficient s_{11} - cardinal directions test.....	33
Fig. 3.15: Radiation pattern - cardinal directions test	34
Fig. 4.1: a) Antenna array with overlapping E-fields (left), b) touching E-fields (middle) and c) distant E-fields (right).....	36
Fig. 4.2: Model of the tuned antenna array	36
Fig. 4.3: Initial scheme of array cable feeding.....	37
Fig. 4.4: Distance between array element feeds.....	38
Fig. 4.5: Antenna array model with applied changes	39
Fig. 4.6: Reflection coefficients s_{11} with and without applied changes	40
Fig. 4.7: Reflection coefficients s_{22} with and without applied changes	40
Fig. 4.8: Creation of constructive and destructive waves	41
Fig. 4.9: Radiation pattern of the 2-element array without tuning (distant elements).....	42
Fig. 4.10: Radiation pattern of the 2-element array without tuning (close elements)	42
Fig. 4.11: Radiation pattern of the tuned 2-element array	43
Fig. 4.12: 3D radiation pattern of the tuned 2-element array	43
Fig. 4.13: Model of 3-element antenna array	44
Fig. 4.14: Reflection coefficient of 3-element and 2-element antenna array	44
Fig. 4.15: Radiation pattern of 3-element and 2-element antenna array	45
Fig. 4.16: 3D Radiation pattern of 3-element antenna array	45
Fig. 4.17: Model of 2-element array with additional coaxial probes	46
Fig. 4.18: Reflection coefficients of 2-element array – functionality test.....	46

Fig. 4.19: Model of the antenna array for cardinal directions test	47
Fig. 4.20: Reflection coefficients s_{11} and s_{22} - cardinal directions test.....	47
Fig. 4.21: Radiation pattern - cardinal directions test	48
Fig. 5.1: Top and side section view of the single antenna	49
Fig. 5.2: Example of drawn patch board.....	50
Fig. 5.3: The fully build single antenna (top view).....	51
Fig. 5.4: Measured and simulated reflection coefficient (100Ω).....	51
Fig. 5.5: Comparison between simulated and measured s_{11} of the new antenna (50Ω)	52
Fig. 5.6: Comparison between simulated and measured s_{22} of the new antenna (100Ω).....	53
Fig. 5.7: 3D Radiation pattern of the newly created antenna	53
Fig. 5.8: Comparison between verified and simulated reflection coefficient (50Ω)	54
Fig. 5.9: Comparison between verified and simulated reflection coefficient (100Ω)	54
Fig. 5.10: 3D Radiation pattern of the verified antenna.....	55

INTRODUCTION

Nowadays, satellite communication is an important part of daily life, in the form of television and mobile broadcasting, navigation, radio channels, fax or the internet [1]. For these technologies and devices, it is mostly appropriate to use the smallest possible receiving or transmitting antennas. However, with small antenna dimensions decreases maximum antenna gain and its efficiency with an increase in attenuation [2].

In this thesis, a compact antenna array is designed and manufactured for communication with the BDSat-2 satellite. The antenna array is primarily created and measured for the city of Brno. The required information about satellite is obtained with the appropriate software. This information is later processed into results of potential gain, and later compared to Longyearbyen, a town in Spitsbergen. Once the results for Brno are obtained and prepared, it'll be possible to determine the type and dimensions of the single antenna, its effective gain at a certain elevation angle and other parameters. The single antenna serves as basis for the creation of the antenna array. Next, the antenna type is selected, designed, modeled and simulated in the program HFSS Ansys. The required antenna results are reflection coefficient and the reflection coefficient, working on required frequency. Once the single antenna is prepared, the antenna array is designed in the same way. Since the goal is to create the antenna array with the lowest dimensions and highest gain possible, multiple tuning methods and another suggestions are presented. Once the array is prepared, the physical model is made and put to the test.

1. STATISTIC

Part of satellite communication is a satellite, which basically represents an antenna or a system of antennas. It moves in its own circular orbit (around the Earth) periodically. In this case, satellite's orbit is analyzed for BDSAT-2 cube satellite (CubeSat in short). Its inclination is 97.5 degrees and its average height is 500km [17].

First, the orbit of the satellite is analyzed for the places where the antenna array will be placed. For comparison, 2 locations the antenna array measurement are considered, and those are Brno, Czech Republic and Longyearbyen, Spitsbergen. For the correct design of the antenna array it is necessary to find out the distance of the satellite from the antenna placement (in this case Brno and Longyearbyen), the period of the satellite in the orbit. From the gathered information it's possible to calculate the potential gain, azimuth and elevation angles of the antenna.

1.1 Data acquisition of satellite position

In order to get the necessary information and data for the satellite, a software will be required. After agreement with the supervisor, the WinListen software from the SatPC32 package is used.

The program reads source files (default from package or custom), that contain Keplerian data in the AMSAT or NASA-2-Line format. It outputs lists in chronological order for any time periods that can be displayed on the screen, printed or stored in a file. The files may contain further text besides the records. Therefore, it is not necessary to edit or modify the files [3]. Main menu of SatPC32 is displayed in Figure 1.1.

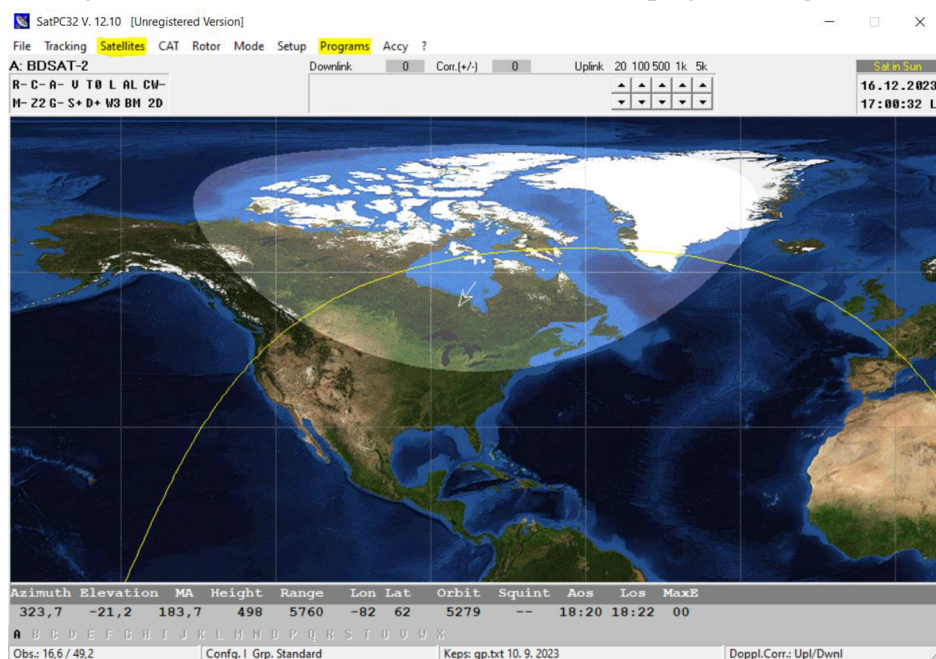


Fig. 1.1: SatPC32 Interface

First, the name and type of satellite for which the data will be acquired must be set. The Kepler data about the satellite are found on the [SATCAT](#) page. After downloading them, the option to choose BDSAT-2 satellite can be set via SatPC32 in the Satellites tab. WinListen can be found in the Programs tab. After starting the WinListen program, it is necessary to first set the geographical latitude and longitude of the place, where the antenna will be located. Next, the BDSAT-2 satellite can be selected from WinListen menu. After selecting the satellite, the date, time interval and period are set. The date and time are set arbitrarily. The interval is set to 5s, meaning new information is obtained every 5s. The period is set to at least 20 days in order to find the period of the satellite's orbit around the selected antenna location (Brno and Longyearbyen have same periods, but the start of the period will be shifted). Useful data are those that have an elevation angle greater than or equal to 0. The data with values lower than 0 are when the satellite is below the horizon. WinListen then outputs all the information about the satellite's position. Acquired data from WinListen are displayed in Figure 1.2. However, the only useful information that can be worked with is day and time, elevation, azimuth and range. The obtained data are exported to a text file for graphic processing.

Day	Time (U)	Azm	Elev	MA	Height	Range	Lon/Lat	Orbit	Squint
17.12.2023	07:45:50	32,4	1,0	178,5	498	2504	44 65	5289	-
17.12.2023	07:45:55	32,9	1,2	178,7	498	2476	44 65	5289	-
17.12.2023	07:46:00	33,4	1,5	179,0	498	2447	43 64	5289	-
17.12.2023	07:46:05	34,0	1,7	179,2	498	2419	43 64	5289	-
17.12.2023	07:46:10	34,5	2,0	179,4	498	2391	43 64	5289	-
17.12.2023	07:46:15	35,1	2,2	179,6	498	2363	43 63	5289	-
17.12.2023	07:46:20	35,7	2,5	179,9	498	2335	42 63	5289	-
17.12.2023	07:46:25	36,3	2,7	180,1	498	2307	42 63	5289	-
17.12.2023	07:46:30	36,9	3,0	180,3	498	2280	42 63	5289	-
17.12.2023	07:46:35	37,6	3,3	180,5	498	2253	42 62	5289	-
17.12.2023	07:46:40	38,2	3,5	180,8	498	2226	42 62	5289	-
17.12.2023	07:46:45	38,9	3,8	181,0	498	2200	41 62	5289	-
17.12.2023	07:46:50	39,6	4,1	181,2	498	2173	41 61	5289	-
17.12.2023	07:46:55	40,3	4,3	181,4	498	2147	41 61	5289	-
17.12.2023	07:47:00	41,0	4,6	181,7	498	2121	41 61	5289	-
17.12.2023	07:47:05	41,7	4,9	181,9	497	2096	41 60	5289	-
17.12.2023	07:47:10	42,5	5,2	182,1	497	2071	40 60	5289	-
17.12.2023	07:47:15	43,2	5,5	182,3	497	2046	40 60	5289	-
17.12.2023	07:47:20	44,0	5,7	182,6	497	2021	40 60	5289	-
17.12.2023	07:47:25	44,8	6,0	182,8	497	1997	40 59	5289	-
17.12.2023	07:47:30	45,6	6,3	183,0	497	1973	40 59	5289	-
17.12.2023	07:47:35	46,5	6,6	183,2	497	1950	40 59	5289	-
17.12.2023	07:47:40	47,4	6,9	183,5	497	1927	39 58	5289	-
17.12.2023	07:47:45	48,3	7,1	183,7	497	1904	39 58	5289	-
17.12.2023	07:47:50	49,2	7,4	183,9	497	1882	39 58	5289	-
17.12.2023	07:47:55	50,1	7,7	184,1	497	1860	39 57	5289	-
17.12.2023	07:48:00	51,1	8,0	184,4	497	1838	39 57	5289	-
17.12.2023	07:48:05	52,0	8,3	184,6	497	1817	39 57	5289	-
17.12.2023	07:48:10	53,0	8,5	184,8	497	1797	38 56	5289	-

(C) DK1TB 2021 QTH1: 16.5 / 49.2 16.12.2023 15:57:24 U

Fig. 1.2: Output data from WinListen program

1.2 Data evaluation

Brno is located in South Moravian region, geographic latitude and altitude for Brno are 49.2253383 and 16.5719524 [4]. Longyearbyen is located on Spitsbergen, the largest

and the only permanently populated island in northern Norway, its latitude and longitude are 78.2229793 and 15.6590955 [5].

Latitude and longitude data are entered into the WinListen program. The period of the satellite's orbit, elevation and azimuth angles, and range from the antenna and satellite location are read from it and extracted into text file. The data of the range are used to determine the path loss. The results of elevation and azimuth are processed into a histogram. With those, it is possible to determine in which position the satellite was most often found. Alternatively, it is also possible to determine the number of antennas for the antenna system and the directivity of the single antenna.

When collecting data, the biggest priority is to find out the maximum angle of elevation for both places. If two or more similar largest values with a similar decrease and increase in elevation are found, then the period can be determined. The satellite's orbit period for the cities of Brno and Longyearbyen is 5 days, which means that in 20 days the satellite can complete its orbit 4 times. However, the number of measured data are much larger for Longyearbyen than for Brno. The reason behind it is that the satellite went over the horizon much more often than in Brno, because Longyearbyen is northern city.

1.2.1 Elevation

The angle of elevation determines the angle formed between the horizontal line and the line of sight. Figure 1.3 shows the angle of elevation between the antenna and satellite. If the line of sight is upward from the horizontal line, then the angle formed is an angle of elevation [6]. In this case, the elevation angle shows the angle that the location of the antenna and satellite makes against the Earth's surface. Only positive elevations are taken into consideration, because of the wasteful, unnecessary radiation of the antenna into the ground.

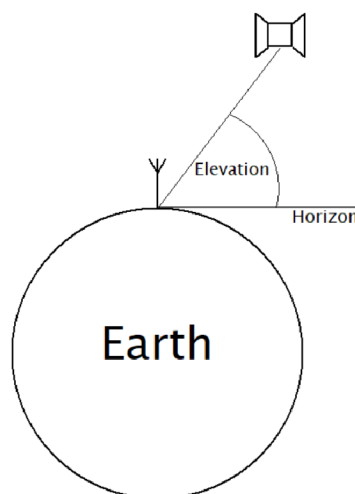


Fig. 1.3: The angle of elevation between the antenna and satellite

Figure 1.4 graphically shows elevation statistics (histogram) for Brno. The histogram was created from 1 period of the satellite's orbit. Individual columns show how many times a certain elevation angle occurred. For example elevation from 0° to 3° occurred 958 times. Columns marked in orange indicate filtered, unnecessary antenna coverage. When the satellite is located directly above the antenna, its gain should be minimal, while at the horizon (minimum elevation angle) maximal. That's why 20% is neglected so that the antenna does not radiate unnecessarily.

Figure 1.5 shows the elevation statistics for Longyearbyen, the measured data are for 1 period as well. Same as with Brno, 20% are neglected. The incidence of low elevations is much greater for Longyearbyen than for Brno, which means that the gain in this direction should be even greater than for Brno. The number of measured data are also greater than for Brno. The main reason is the northern location of the city, where the satellite rises above the horizon much more often.

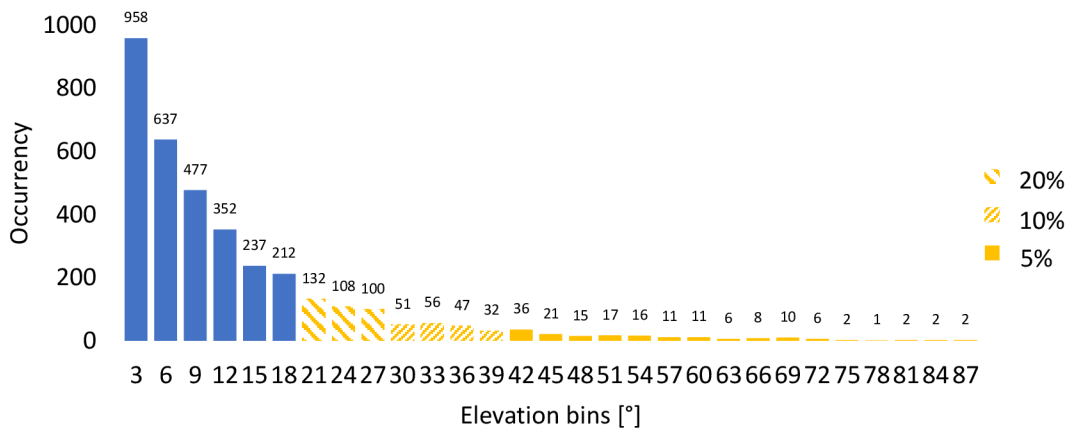


Fig. 1.4: Histogram of elevation for Brno

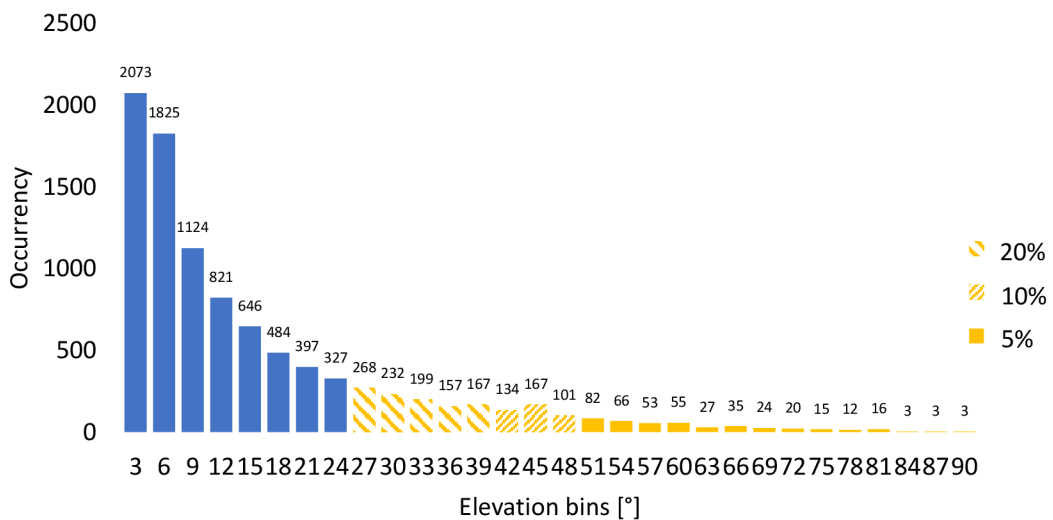


Fig. 1.5: Histogram of elevation for Longyearbyen

1.2.2 Azimuth

Azimuth is direction, measured in degrees clockwise from north on an azimuth circle, which consists of 360 degrees. East corresponds to 90 degrees, south corresponds to 180 degrees, west is 270 degrees, and 360 degrees or 0 degrees north [7]. Brief example of the angle of azimuth of the antenna and the satellite can be seen in Figure 1.6.

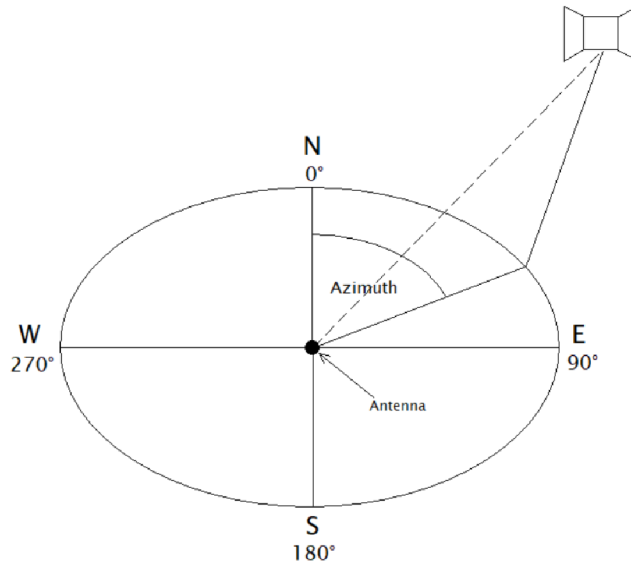


Fig. 1.6: The angle of azimuth of the antenna and the satellite

The south angle (180 degrees) for the city of Brno appears on the histogram 86 times, this can be observed in the histogram, Figure 1.7. Since the radiation of the antenna in the opposite direction is unwanted, 20% of the azimuth angles for Brno (from 130 degrees to 210 degrees) are filtered out. After filtering, the histogram shows that one or two antennas will be needed (blue part of the histogram). The first antenna would radiate with coverage from 10 degrees to 120 degrees (north to south-east), and the second antenna would radiate with coverage from 220 degrees to 360 degrees (south-west to north).

Same as with Brno, the azimuth histogram for Longyearbyen is considered with 20% filtering. The histogram of the azimuth of Longyearbyen is shown in Figure 1.8. As mentioned before in subsection 1.2.1 with the elevations, the satellite rises above the horizon much more often than in Brno, so the number of measured data are significantly larger. The satellite will most often be found at 40 degrees (north-east) and 330 degrees (north-west), which means that in this case it is possible to use two antennas.

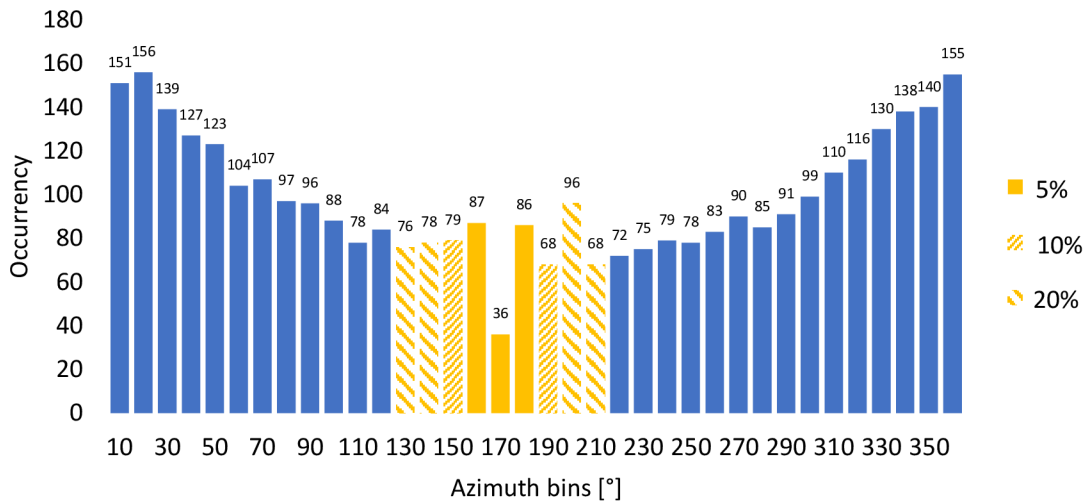


Fig. 1.7: Histogram of azimuth for Brno

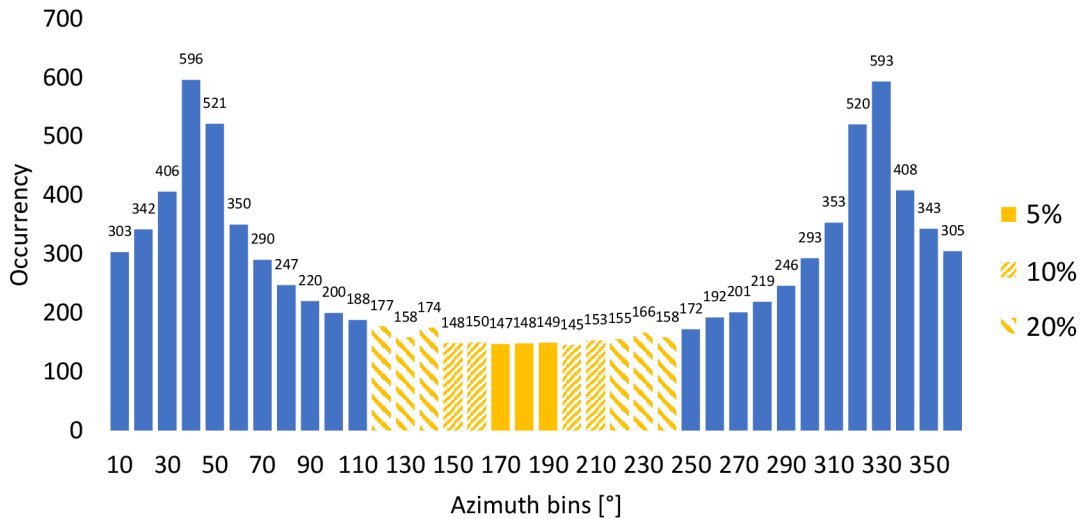


Fig. 1.8: Histogram of azimuth for Longyearbyen

1.2.3 Gain

As mentioned in the previous subsections, the required antenna must be designed with the highest gain possible in mind. To put it in the perspective of the satellite, the highest gain must be, when the satellite is on the horizon. In this case, the angle of elevation ~ 0 degrees. With increasing elevation, its gain is decreasing. Because the Earth is round, graphs for Brno and Longyearbyen are same.

Attenuation by propagation depends on the distance, and the distance depends on the circular path of the satellites. Formula (1.1) tells how to calculate a maximal range attenuation dependent on elevation at horizon. This formula (1.2) can be used for the rest of the elevations. To calculate a range gain, a calculated attenuation for a certain

elevation below maximal needs to be subtracted from the maximal value (1.3). The data about range between the satellite and the antenna placement are acquired from the SatPC32.

$$Att_{max} = 20 \cdot \log(range_{elv=0}) = 20 \cdot \log(2682) = 68.57dB \quad 1.1$$

$$Att_{elv=5} = 20 \cdot \log(range_{elv=5}) = 20 \cdot \log(2142) = 66.62dB \quad 1.2$$

$$Gain_{elv=5} = Att_{max} - Att_{elv=5} = 68.57 - 66.62 = 1.95dB \quad 1.3$$

Semi-circular shape of the graph in Figure 1.9 proves, that the satellite is indeed floating in circular manner. The higher the satellite is above horizon, the closer it gets to the antenna location, thus the potential gain increases when the satellite gets closer and closer to 90 degrees.

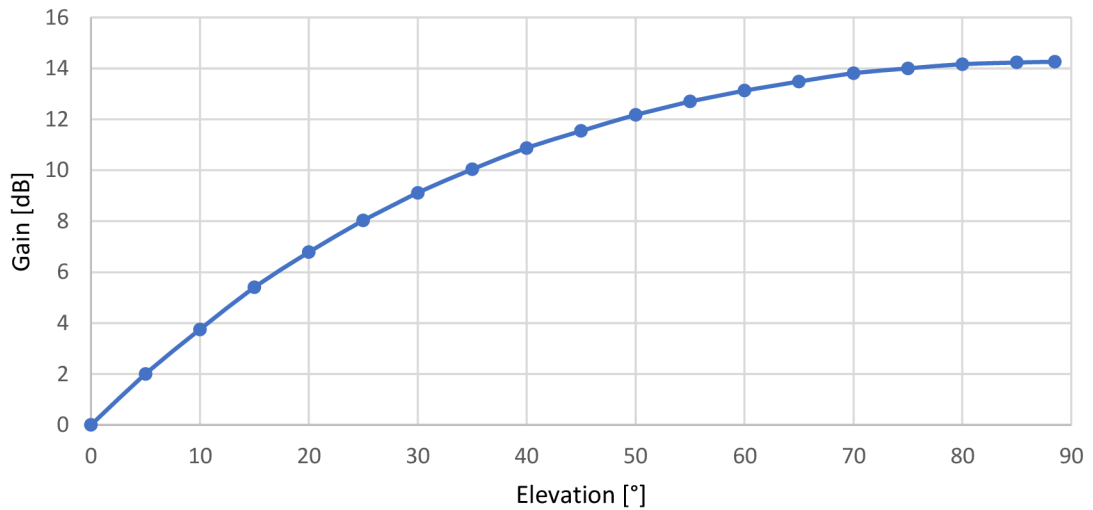


Fig. 1.9: Potential gain for Brno and Longyearbyen

Based on the data from the Figure 1.9, the ideal radiation pattern of the antenna is shown in Figure 1.10, but only its vertical elevation section. The ideal radiation pattern shows the ideal behavior of the antenna, which radiates no power back (in the opposite direction) or below the horizon.

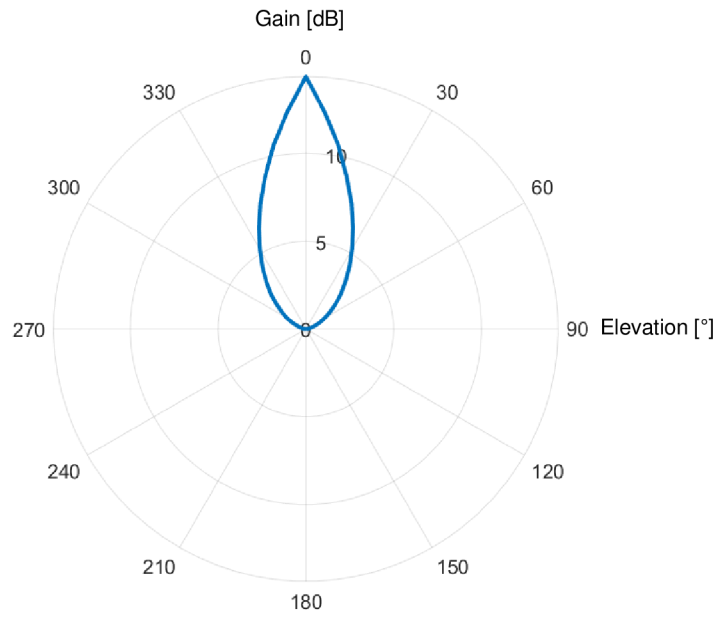


Fig. 1.10: Ideal radiation pattern of the antenna (vertical section - elevation)

2. ANTENNA DESIGN

After obtaining the necessary data, it is possible to start with the design of single antenna, which will serve as basis for the antenna system. After agreement with the supervisor, the designed antenna is a patch square antenna with coaxial feeding. The parameters of the antenna, which were agreed upon as well, are resonant frequency $f_0 = 436.5\text{MHz}$ and bandwidth from 435MHz to 438MHz . The bandwidth (measured at $S_{11} = -10\text{dB}$) must be greater than 3MHz mainly because of tolerances, involving dimensions, temperature, etc.

2.1 Dielectric substrate

The dielectric substrate must meet the following conditions. The material's permittivity must be as large as possible and the color of the material must be white or yellow. Dark colored substrates contain carbon, which can cause unexpected and unwanted losses. Also it must not be very hard, like for example ceramic plates, otherwise the production would be too complicated. Usually such materials have large relative permittivity above 4. Usable materials for antenna design have relative permittivity around 4. Below, in upcoming subsections, are shown 3 acceptable examples.

2.1.1 FR4

FR-4 or Flame Retardant Glass Epoxy consists of woven fiberglass and a flame-retardant epoxy resin. It's often used as an insulator in dry or humid conditions or in this case a dielectric substrate [8]. Its relative permittivity ranges from 3.8 to 4.8. Depending on the glass weave style, thickness, resin content, and copper foil roughness, the relative permittivity can go even higher [9]. Although the substrate has excellent dielectric properties, it is not possible to use it in the design of the antenna due to its changing properties in humid conditions.

2.1.2 Nylatron

Nylatron is from a family of nylon plastics filled with molybdenum disulfide lubricant powder. It is used to cast plastic parts for machines, because of its mechanical properties and wear-resistance or in electronic is used as an insulator [10]. In this case, Nylatron can be considered as a dielectric substrate. Currently on market are 3 different types of Nylatron: Nylatron GS, Nylatron GSM, and Nylatron NSM. For all types relative permittivity is from 3.2 to 3.7 for 1MHz and higher [11]. This type of substrate is a suitable choice for antenna design, but not the best and safest option, hence the relative permittivity could be a little bit higher and some variations have darker colors.

2.1.3 Ertalon 6

Ertalon 6 SA (White) or PA (Black) is a heat stabilised cast nylon grade, which exhibits a great combination of mechanical strength, stiffness, mechanical damping properties, toughness, and wear resistance. In addition, this particular grade possesses excellent electrical insulating properties [12]. For Ertalon 6 SA and Ertalon 6 PA, the relative permittivity is from 3.3 to 3.8 for 1MHz and higher [13]. For this antenna design, Ertalon 6 SA will be a suitable choice because of its white color (no carbon in the structure) and for its relative permittivity. That is why Ertalon 6 SA will be used for further calculations and antenna design.

2.2 Dimensions of square patch

In this chapter, the parameters and dimensions are designed and calculated for a square patch antenna fed by coaxial cable, shown in Figure 2.1. The parameters of the proposed antenna are L_{sub} , L and h , where L_{sub} is the length of the substrate, L is the length of the square patch and h is the height of the substrate. Patch to ground pin serves for connecting those two components.

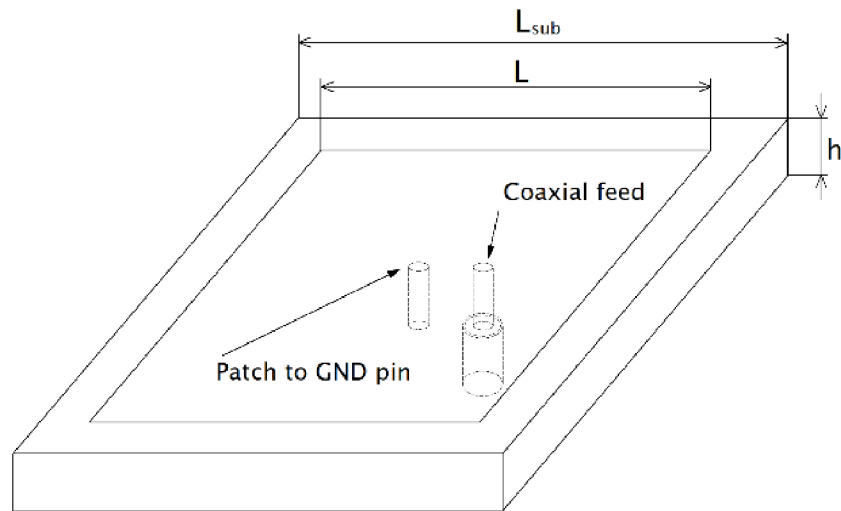


Fig. 2.1: Square Patch antenna with coaxial feeding

First of all, the height of the substrate h must be found. According to (2.2), it is possible to find in what range the height is located. The specified height h must be much smaller than the center wavelength λ_0 ($h \ll \lambda_0$). The wavelength is calculated in (2.1), the result is then used in (2.2) [14].

$$\lambda_0 = \frac{c_0}{f_0} = \frac{3 \cdot 10^8}{436,5 \cdot 10^6} = 687,3mm \quad 2.1$$

$$0,003 \cdot \lambda_0 < h < 0,05 \cdot \lambda_0$$

The height of the substrate $h = 15\text{mm}$ is a suitable choice, since it is within calculated the range from 0.21mm to 34.37mm .

After verifying the height of the substrate h , it is possible to start calculating the dimensions of the square patch. The width of the patch W and the length of the patch L are the same, because the patch is a square ($W = L$). In order to obtain an accurate result, two iterations are used where, for example, the resulted L_0 from 0^{th} iteration is placed as W_1 in 1^{st} iteration. To summarize taken steps, first, the width W of square patch is calculated (2.3), then after determining the patch width, the relative effective permittivity (2.4) of the substrate ϵ_{reff} is determined. Then the extension ΔL is calculated (2.5) and last the length of the patch L (2.6). This entire procedure is repeated from zero to the second iteration [14].

0^{th} iteration:

$$W_0 = \frac{c_0}{2 \cdot f_r} \cdot \sqrt{\frac{2}{\epsilon_r + 1}} = \frac{3 \cdot 10^8}{2 \cdot 436.5 \cdot 10^6} \cdot \sqrt{\frac{2}{3.8 + 1}} = 222 \cdot 10^{-3} \text{m} = 222 \text{mm} \quad 2.3$$

$$\epsilon_{\text{reff}0} = \frac{\epsilon_r + 1}{2} + \frac{\epsilon_r - 1}{2} \left(1 + 12 \frac{h}{W_0}\right)^{-\frac{1}{2}} = \frac{3.8 + 1}{2} + \frac{3.8 - 1}{2} \left(1 + 12 \frac{15 \cdot 10^{-3}}{222 \cdot 10^{-3}}\right)^{-\frac{1}{2}} = 3.44 \quad 2.4$$

$$\Delta L_0 = 0.412 \cdot h \cdot \frac{(\epsilon_{\text{reff}0} + 0.3) \left(\frac{W_0}{h} + 0.264\right)}{(\epsilon_{\text{reff}0} - 0.258) \left(\frac{W_0}{h} + 0.8\right)} = 0.412 \cdot 0.015 \cdot \frac{(3.44 + 0.3) \left(\frac{222 \cdot 10^{-3}}{15 \cdot 10^{-3}} + 0.264\right)}{(3.44 - 0.258) \left(\frac{222 \cdot 10^{-3}}{15 \cdot 10^{-3}} + 0.8\right)} \quad 2.5$$

$$\Delta L_0 = 7.014 \cdot 10^{-3} \text{m}$$

$$L_0 = \frac{c_0}{2 \cdot f_r \cdot \sqrt{\epsilon_{\text{reff}0}}} - 2 \cdot \Delta L_0 = \frac{3 \cdot 10^8}{2 \cdot 436.5 \cdot 10^6 \cdot \sqrt{3.44}} - 2 \cdot 7.014 \cdot 10^{-3} \quad 2.6$$

$$L_0 = 171.25 \cdot 10^{-3} \text{m} = 171.25 \text{mm}$$

1^{st} iteration:

$$L_0 = W_1$$

$$\epsilon_{\text{reff}1} = \frac{\epsilon_r + 1}{2} + \frac{\epsilon_r - 1}{2} \left(1 + 12 \frac{h}{W_1}\right)^{-\frac{1}{2}} = \frac{3.8 + 1}{2} + \frac{3.8 - 1}{2} \left(1 + 12 \cdot \frac{15 \cdot 10^{-3}}{171.25 \cdot 10^{-3}}\right)^{-\frac{1}{2}} = 3.38$$

$$\Delta L_1 = 0.412 \cdot h \cdot \frac{(\varepsilon_{reff1} + 0.3) \left(\frac{W_1}{h} + 0.264 \right)}{(\varepsilon_{reff1} - 0.258) \left(\frac{W_1}{h} + 0.8 \right)} = 0.412 \cdot 0.015 \cdot \frac{(3.38 + 0.3) \left(\frac{171.25 \cdot 10^{-3}}{15 \cdot 10^{-3}} + 0.264 \right)}{(3.38 - 0.258) \left(\frac{171.25 \cdot 10^{-3}}{15 \cdot 10^{-3}} + 0.8 \right)}$$

$$\Delta L_1 = 6.966 \cdot 10^{-3} m$$

$$L_1 = \frac{c_0}{2 \cdot f_r \cdot \sqrt{\varepsilon_{reff1}}} - 2 \cdot \Delta L_1 = \frac{3 \cdot 10^8}{2 \cdot 436.5 \cdot 10^6 \cdot \sqrt{3.38}} - 2 \cdot 6.965 \cdot 10^{-3}$$

$$L_1 = 172.97 \cdot 10^{-3} m = 172.97 mm$$

2nd iteration:

$$L_1 = W_2$$

$$\varepsilon_{reff2} = \frac{\varepsilon_r + 1}{2} + \frac{\varepsilon_r - 1}{2} \left(1 + 12 \frac{h}{W_2} \right)^{-1/2} = \frac{3.8 + 1}{2} + \frac{3.8 - 1}{2} \left(1 + 12 \cdot \frac{15 \cdot 10^{-3}}{173 \cdot 10^{-3}} \right)^{-1/2} = 3.38$$

$$\Delta L_2 = 0.412 \cdot h \cdot \frac{(\varepsilon_{reff2} + 0.3) \left(\frac{W_2}{h} + 0.264 \right)}{(\varepsilon_{reff2} - 0.258) \left(\frac{W_2}{h} + 0.8 \right)} = 0.412 \cdot 0.015 \cdot \frac{(3.38 + 0.3) \left(\frac{173 \cdot 10^{-3}}{15 \cdot 10^{-3}} + 0.264 \right)}{(3.38 - 0.258) \left(\frac{173 \cdot 10^{-3}}{15 \cdot 10^{-3}} + 0.8 \right)}$$

$$\Delta L_2 = 6.968 \cdot 10^{-3} m$$

$$L_2 = \frac{c_0}{2 \cdot f_r \cdot \sqrt{\varepsilon_{reff2}}} - 2 \cdot \Delta L_2 = \frac{3 \cdot 10^8}{2 \cdot 436.5 \cdot 10^6 \cdot \sqrt{3.38}} - 2 \cdot 6.968 \cdot 10^{-3}$$

$$L_2 = 172.98 \cdot 10^{-3} m = 172.98 mm$$

After calculating the final patch length from the 2nd iteration, all antenna parameters are ready for simulation in the HFSS Ansys program (more in chapter 3).

2.3 Coaxial feed and impedance on the edge

The single square patch antenna is fed by coaxial cable. The inner conductor of the coaxial cable is connected to a square patch, or in another word, a radiator. However, the coaxial feed cannot be placed into the patch in any place. The reason is the different impedance at the point of antenna feed. For example, the impedance of the feed (coaxial cable) near the center of the patch (really close to the center pin) would be very low, while at the edge it would be maximal. To match the impedance to 50Ω , the formulas for calculating the patch edge impedance (2.9) and calculating the distance x_0 at 50Ω

input impedance (2.10) must be used [14]. Lastly, distance x_1 (2.11), the distance from the center of the antenna, is calculated. The whole process of coaxial probe placement is displayed in Figure 2.2.

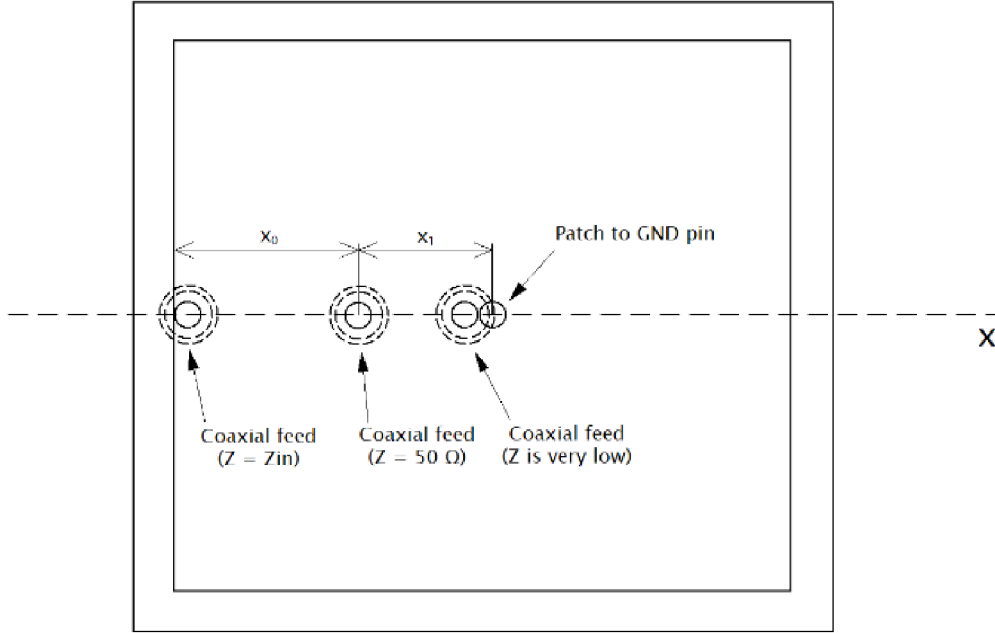


Fig. 2.2: Coaxial feed in 3 different positions (TOP side)

To find the required distance, the conductance and impedance at the edge of the patch must be calculated first. Conductivity G_1 is calculated according to (2.8), where $W = L$ and k_0 , a free space wave number, is calculated according to (2.7). After determining the conductivity, the impedance at the edge of the patch (2.9) is calculated, the value of which is 240Ω . Finally, the value of the distance x_0 is calculated at an input impedance of 50Ω (2.10) [14].

$$k_0 = \frac{2 \cdot \pi}{\lambda_0} = \frac{2 \cdot \pi}{687.3 \cdot 10^{-3}} = 9.14 m^{-1} \quad 2.7$$

$$G_1 = \frac{W}{120 \cdot \lambda_0} \left[1 - \frac{1}{24} (k_0 \cdot h)^2 \right] = \frac{172.98 \cdot 10^{-3}}{120 \cdot \lambda_0} \left[1 - \frac{1}{24} (9.14 \cdot 10 \cdot 10^{-3})^2 \right] \quad 2.8$$

$$G_1 = 2.09 \cdot 10^{-3} mS$$

$$Z_{IN}(x_0 = 0) = \frac{1}{2 \cdot G_1} = \frac{1}{2 \cdot 2.12 \cdot 10^{-3}} = 240\Omega \quad 2.9$$

$$x_0 = \frac{L}{\pi} \cdot \cos^{-1} \left(\sqrt{\frac{Z_{IN}(x = x_0)}{Z_{IN}(x = 0)}} \right) = \frac{172.98 \cdot 10^{-3}}{\pi} \cdot \cos^{-1} \left(\sqrt{\frac{50}{240}} \right) \quad 2.10$$

$$x_0 = 60.39 \cdot 10^{-3}m = 60.39mm$$

$$x_1 = \frac{L}{2} - x_0 = \frac{172.98 \cdot 10^{-3}}{2} - 60.39 \cdot 10^{-3} \quad 2.11$$

$$x_1 = 26.1 \cdot 10^{-3}m = 26.1mm$$

The value of the distance x_1 is 26.1 mm from the edge of the patch. Calculation is simplified and neglects all losses. This value is used as basis when modeling the antenna in the simulator and it might slightly change when tuning the antenna (more in 3rd chapter).

3. SINGLE ANTENNA

In this chapter, the square patch antenna fed by a coaxial cable is modeled and tuned in the HFSS Ansys program. The antenna is simulated in free space, the calculated dimensions of the patch and coaxial probe feed from the 2nd chapter are applied when modeling the antenna. After drawing the antenna, the reflection coefficient s_{11} is tuned to the specified frequency $f_0 = 436.5\text{MHz}$, then the bandwidth at the value of the reflection coefficient -10dB must be found. The radiation pattern of the antenna must be drawn in order to determine, whether it is necessary to suppress side lobes and back lobe or to boost the maximum gain of the antenna in the desired direction (main lobe).

3.1 Antenna modeling

The basic square patch antenna is displayed in Figure 3.1. First, the substrate is modeled in the shape of a square cuboid. Below the substrate is drawn the ground plane GND with the same x and y dimensions as the substrate and above it is modeled a square patch according to the calculated dimensions from 2nd chapter ($L = 172.98\text{mm}$). The ground plane is made out of copper with a thickness of 0.5mm . The copper center pin that connects GND and the patch has a diameter of 6mm and is made out of copper as well. The coaxial cable consists of 3 cylinders 20mm high. The inner conductor of the coaxial line is 10mm longer (it touches the patch). The diameter of the inner conductor is 1mm (Copper), the diameter of the dielectric insulator is 5mm (Teflon) and the coaxial shield has a diameter of 5.5mm (Copper). Excitation of the coaxial probe consists of wave port with input impedance 50Ω . The entire antenna is surrounded by a square air cube with dimensions of $600 \times 600 \times 600\text{mm}$. The walls of the air cube are marked as radiating, without it the simulation wouldn't run. After drawing the air cube, the model is ready for simulation and further testing.

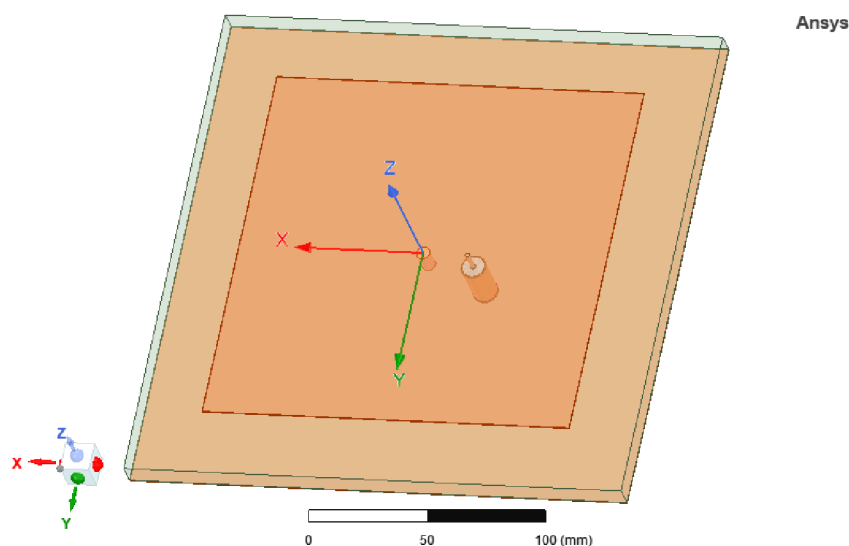


Fig. 3.1: Modeled square patch antenna in HFSS Ansys

3.1.1 Impedance change

First of all, in the HFSS Ansys simulator, wave port must be set to 50Ω , otherwise it's not going to work. Secondly, a new dielectric material with correct dimensions must be assigned to coaxial probe. Relation (3.1) is for calculation of the coaxial cable impedance [22]. Since the impedance is already known, the (3.1) is used to calculate the dielectric outer diameter. For modeling and design purposes, the dielectric insulation is stays as Teflon, which its relative permittivity is equal to 2.1.

$$Z_0 = \frac{138 \cdot \log_{10} \left(\frac{D_d}{D_c} \right)}{\sqrt{\epsilon_r}}$$

Relation (3.2) shows full calculation of the dielectric outer diameter of the coaxial probe (50Ω), where D_c is diameter of inner conductor and D_d is required diameter of dielectric insulator.

$$D_d = 10^{\frac{Z_0 \cdot \sqrt{\epsilon_r}}{138}} \cdot D_c = 10^{\frac{50 \cdot \sqrt{2.1}}{138}} \cdot 1 \cdot 10^{-3} = 3.4mm \quad 3.2$$

For the whole array element feeding design to function as intended, the antenna impedance must be matched to 100Ω , as it's shown in Figure 4.3. Since the single antenna and the antenna array also meant for 100Ω , the diameter of the dielectric insulator is calculated as well. Its value is 11.2mm. After the diameter of dielectric insulator is calculated and applied in the simulator, a new position for coaxial feed must be found. By using (2.10) and (2.11) from chapter 2.3, a new position of coaxial from the center of the patch is 39.7mm.

$$D_d = 10^{\frac{Z_0 \cdot \sqrt{\epsilon_r}}{138}} \cdot D_c = 10^{\frac{100 \cdot \sqrt{2.1}}{138}} \cdot 1 \cdot 10^{-3} = 11.2mm$$

3.2 Experimenting with antenna dimensions

The main goal is to achieve the highest gain possible with only one patch antenna while maintaining reasonable antenna dimensions. The antenna is tuned by changing the dimensions of dielectric substrate height, ground plane and patch.

3.2.1 Dependence of the height on bandwidth and gain

A different height of a substrate from calculated range 0.21mm to 34.37mm (chapter 2) might have influence on results. Although the range of substrate height is determined, properties of the dielectric substrate must be taken into consideration like for example weight or sturdiness. Therefore, the mentioned range must be limited to more realistic scale. Going below calculated range would resolve in low total gain and

bandwidth, while going above the calculated range would resolve in excessive weight and dimensions.

Figure 3.2 shows a relation between bandwidth and height of the substrate. With increasing height increases bandwidth almost linearly, but the resonant frequency decreases. Going for lower value, like 5mm, can result in a bandwidth smaller than 3MHz, while going for higher value, like 20mm, can result in unnecessary dimension, though only minimal. As the most optimal choice, the height of 15mm still remains. In figure 3.3, total gain increases with increasing substrate height. Although the highest gain achieved is for 20mm, the total gain is increased only by 0.1dB from 15mm. Hence the final chosen height of dielectric substrate is 15mm.

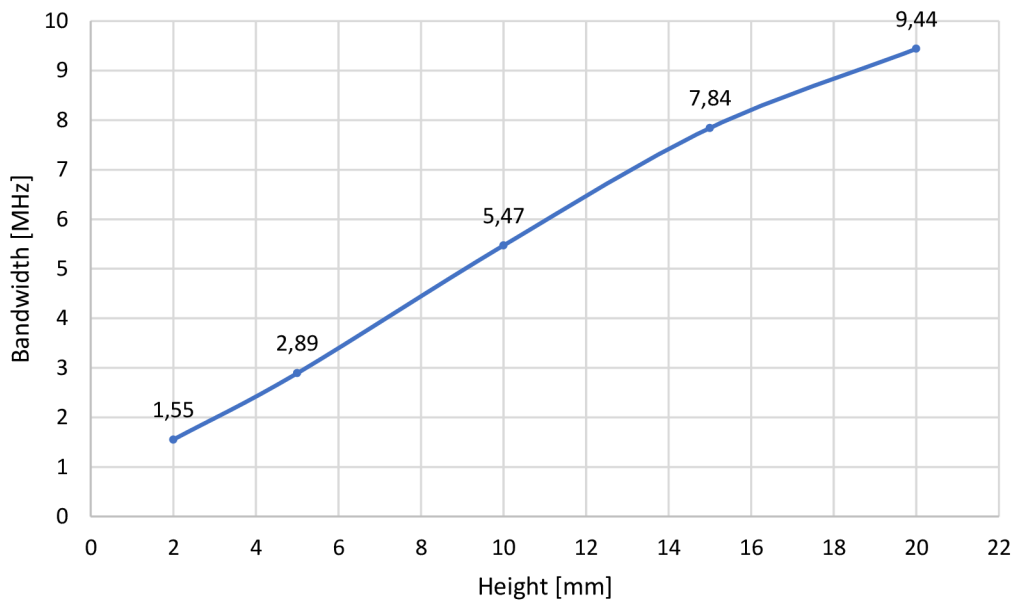


Fig. 3.2: Dependence of the bandwidth on the substrate height

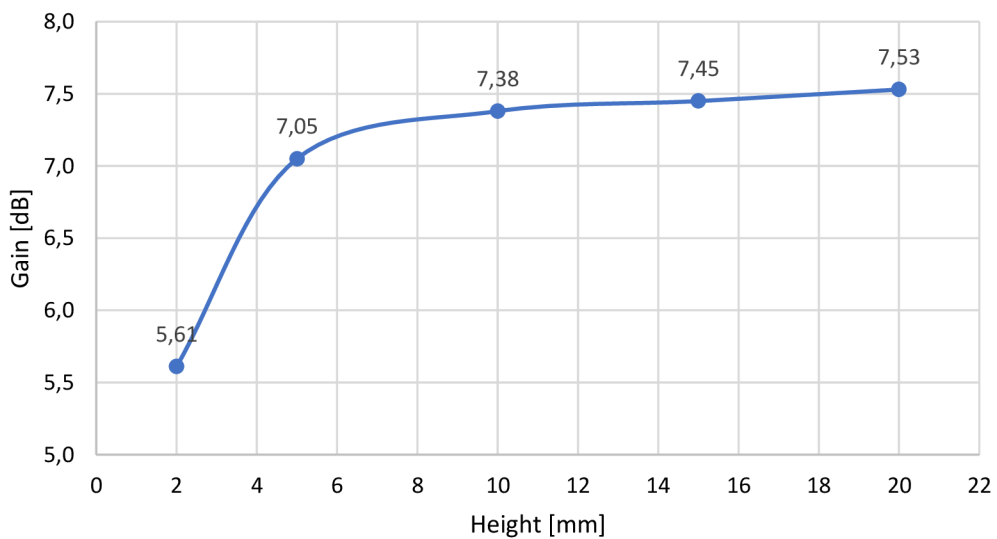


Fig. 3.3: Dependence of the total gain on the substrate height

3.2.2 Dependence of the ground plane on antenna gain

By leaving the ground plane as wide as the antenna substrate itself (Figure 3.1), the total gain is minimal and the antenna is unusable in this state. By expanding the ground plane of the antenna, it is possible to achieve much higher total gain. Dependence of the gain on the ground plane length of the antenna is displayed in Figure 3.4.

The main goal is to choose a ground plane dimension with the most optimal total gain value. Going too low might cause the total gain being too low, hence the antenna would be unusable. By going for the highest total gain value, the ground plane would be too wide, causing the antenna to be impractical and ineffective. Therefore, the optimal ground plane range is from 350mm to 400mm. The chosen ground plane dimension is 390mm.

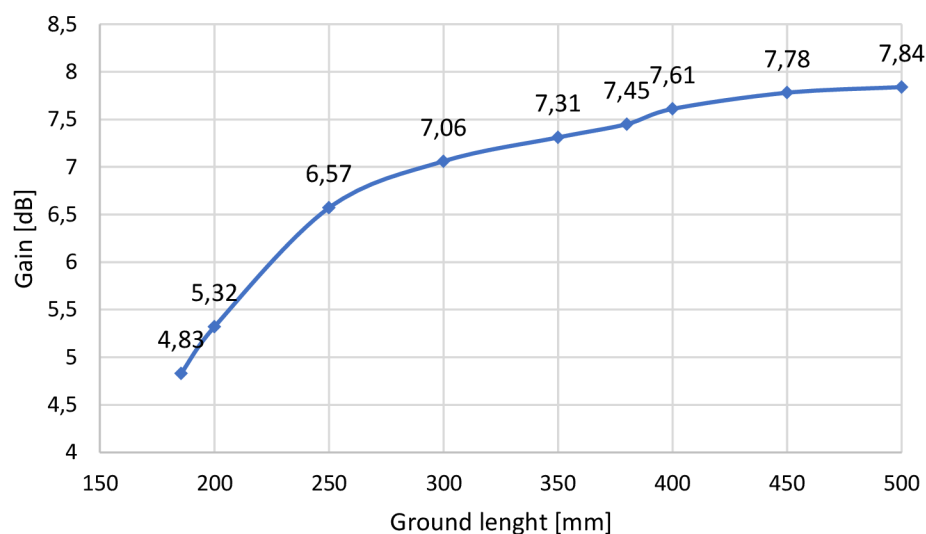


Fig. 3.4: Dependence of the gain on the ground length of the antenna

3.3 Reflection coefficient

Reflection coefficient s_{11} shows how much power is reflected from the antenna. All the power from the antenna is reflected and nothing is radiated if the s_{11} is approximately 0dB [15].

Figure 3.5 shows the characteristic of the reflection coefficient s_{11} tuned at a frequency of 436.5MHz. The calculated dimensions from the previous chapters do not guarantee an immediate result, but serve only as a guide. Changing the dimensions of the substrate, the ground plane, the patch and changing the position of coaxial feed will have effects on the tuning. For example, when changing the position of coaxial feed, the impedance of the single antenna changes as well, and with that, the value of the reflection coefficient s_{11} changes as well. Figure 3.6 shows reflection coefficient of the single antenna tuned to 50Ω.

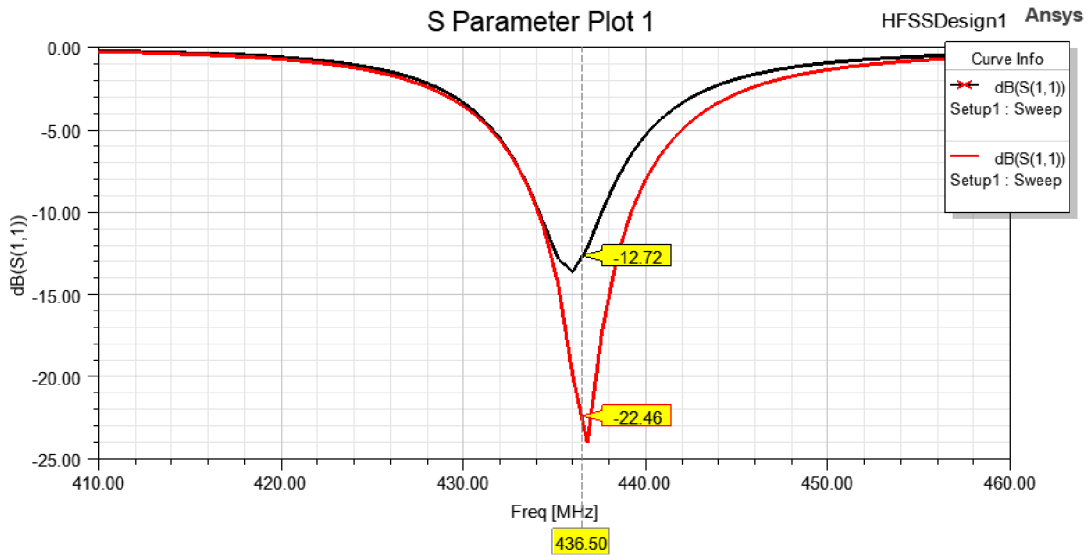


Fig. 3.5: Reflection coefficient s_{11} with different position of coaxial feed

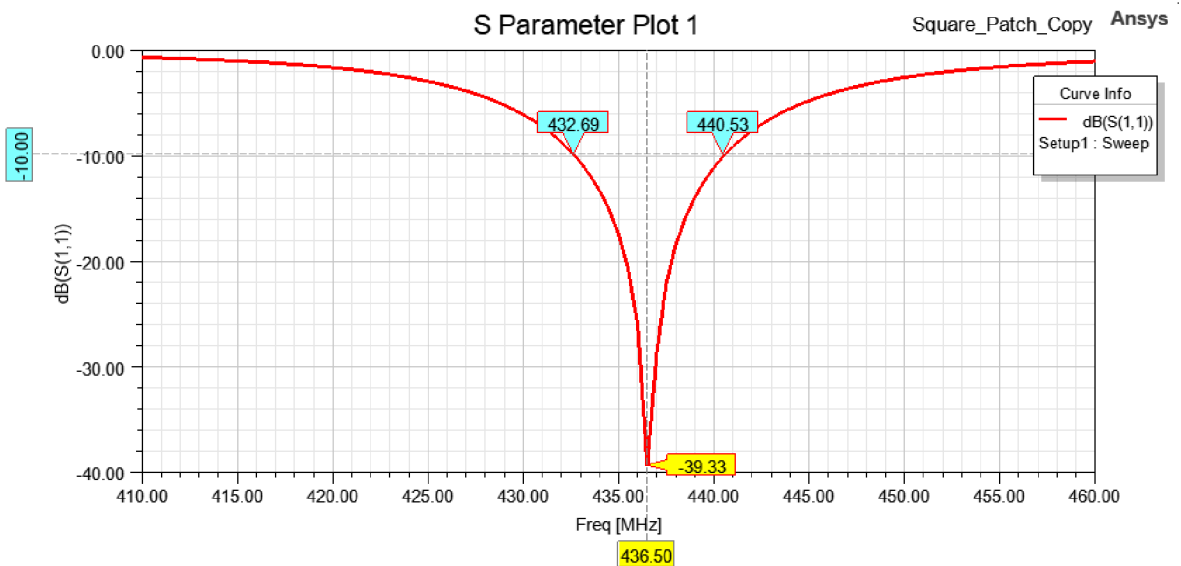


Fig. 3.6: Reflection coefficient s_{11} and bandwidth of the tuned antenna

After changing the dimensions of the ground plane in order to achieve the maximum gain (more about that in chapter 3.4), the resonance at given frequency is achieved with bandwidth of 7.84MHz, frequency band from 432.69MHz to 440.53MHz at -10dB, and value of reflection coefficient $s_{11} = -39.33$ dB. This can be seen in Figure 3.6. The length of a patch was changed as well from 174.88mm to 169mm to help achieve minimal reflection coefficient s_{11} at given resonant frequency.

3.4 Radiation pattern

Radiation pattern is a directional or angular dependence of the power of radio waves from the antenna. It is usually shown in a polar coordination system, either as 2D or 3D. The important parameters of the radiation pattern are lobes of the antenna. Those are

main lobe, side lobes, minor lobes and back lobe. The main lobe shows the wanted direction of antenna radiation. The other lobes are unwanted radiation that must be suppressed or ideally completely eliminated [16].

Gain of the antenna is adjusted by increasing the length of the ground plane or decreasing the length of the patch. If the dimensions of the patch and the ground plane are the same, a large part of the power radiates back (180 degrees), which causes the radiation pattern to look like number 8. This can be seen in Figure 3.8. The larger the ground plane, the more gain increases up to the maximum value. As mentioned before, the right found dimension for the ground plane is 390mm. Figure 3.7 show the model of single antenna with increased size of the ground plane. By increasing the length of the ground plane, the back lobe is more suppressed, but widening the ground plane too much will lead to inefficient usage of space and undesired overall length.

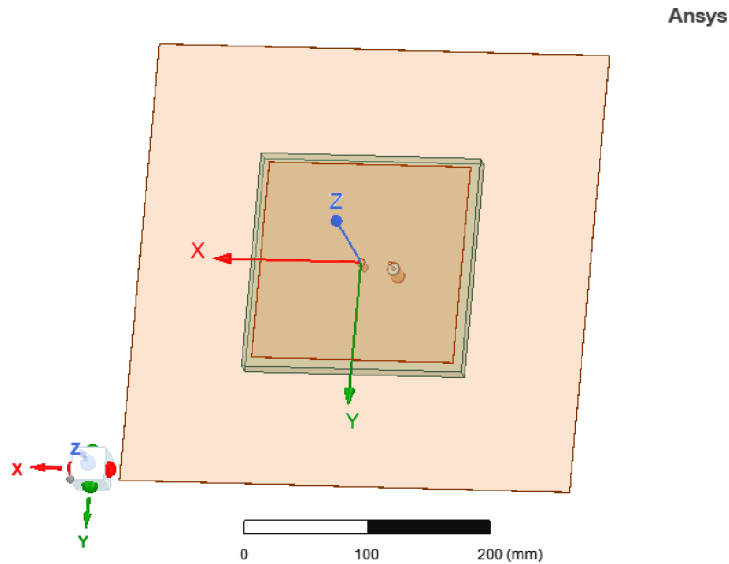


Fig. 3.7: Square patch antenna with expanded ground plane

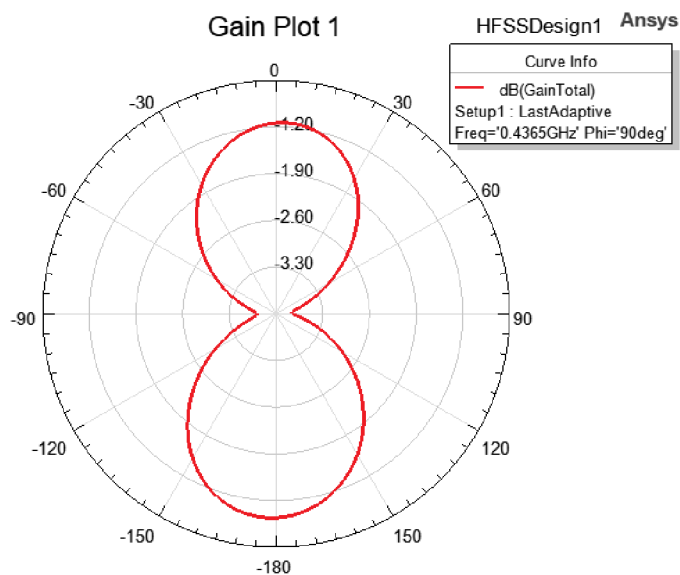


Fig. 3.8: Radiation pattern of the antenna – E-plane (GND and patch are same)

In summary, the found length of the ground plane is 390mm and the length of the patch is 169mm. Maximum acceptable gain of the antenna is around 6.27dB, displayed on 2D radiation pattern (Figure 3.9) and 3D radiation pattern (Figure 3.10). Unwanted side lobes are suppressed completely and the back lobe is suppressed as much as possible.

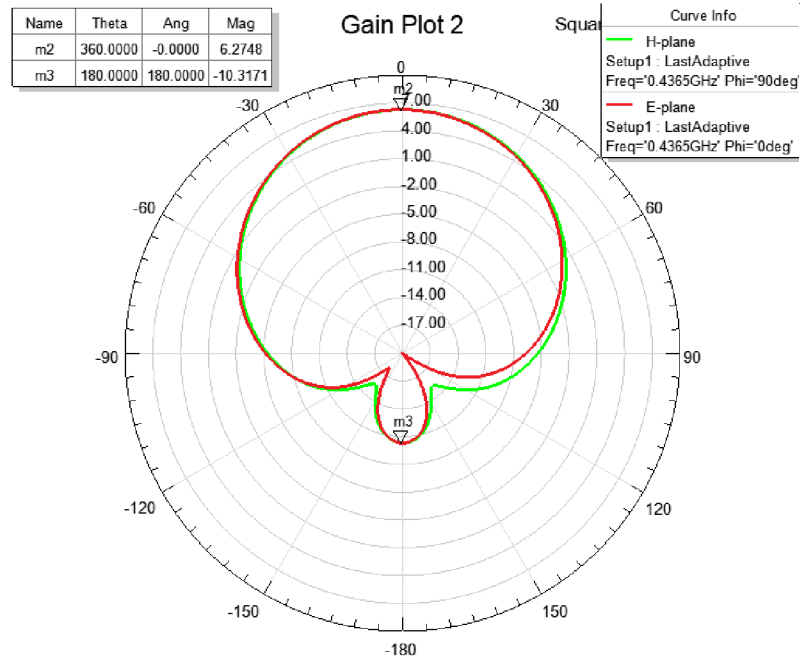


Fig. 3.9: Radiation pattern of the square patch antenna – E-plane

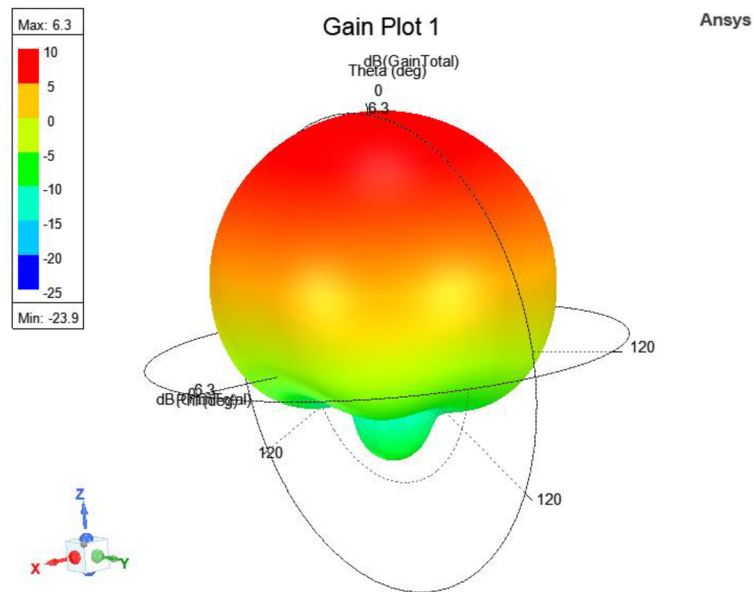


Fig. 3.10: 3D gain plot of the square patch antenna

3.5 Verification of single antenna

Now that the whole antenna design is optimized and prepared, it is possible to verify functionality of the design by adding another (secondary) coaxial feed on x-axis with the same distance from the middle of the antenna as the first one. The single antenna with vertical and horizontal polarization is displayed in Figure 3.11.

In Figure 3.12, both reflection coefficients s_{11} and s_{22} are displayed. Since both reflection coefficients are overlapping each other with a small shift in frequency, it's safe to say that antenna works as intended.

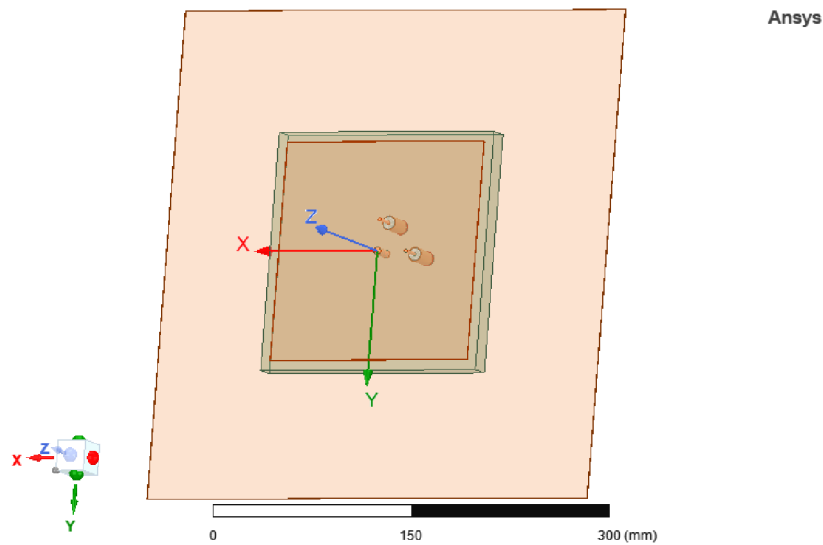


Fig. 3.11: Square patch antenna with 2 coaxial probes

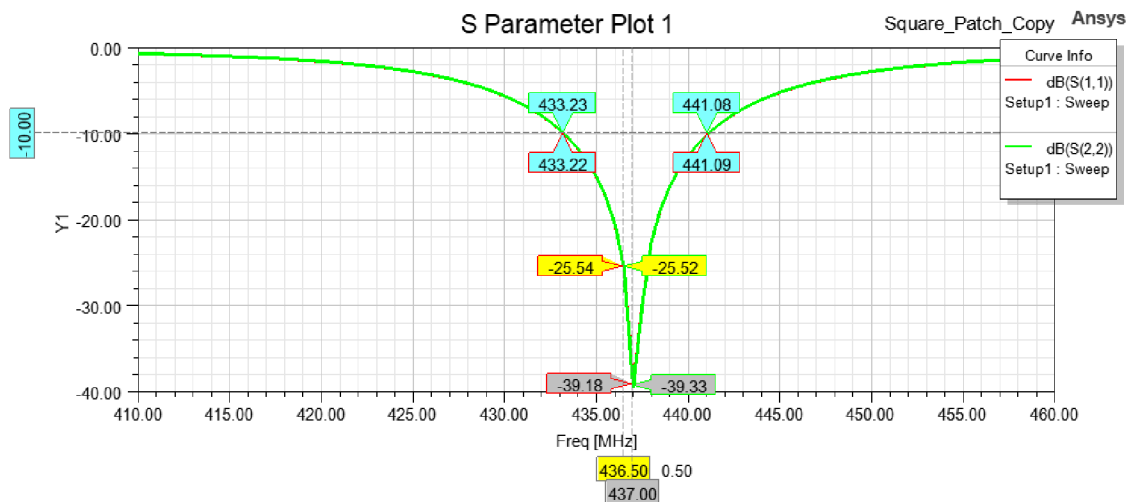


Fig. 3.12: Reflection coefficients of the antenna – functionality test

Figure 3.13 shows another way of checking the antenna functionality. By adding another 3 ground planes placed in a square formation, it's possible to simulate an antenna behavior in case of radiation in all main directions. The reflection coefficient, displayed in figure 3.14, has increased almost by 10dB, while total gain on radiation

pattern displayed in figure 3.15 has decreased by around 0.5dB. Although there are some differences in results, the resonant frequency from Figure 3.14 didn't change and radiation pattern from Figure 3.15 is similar to figure 3.9, hence the antenna works as intended.

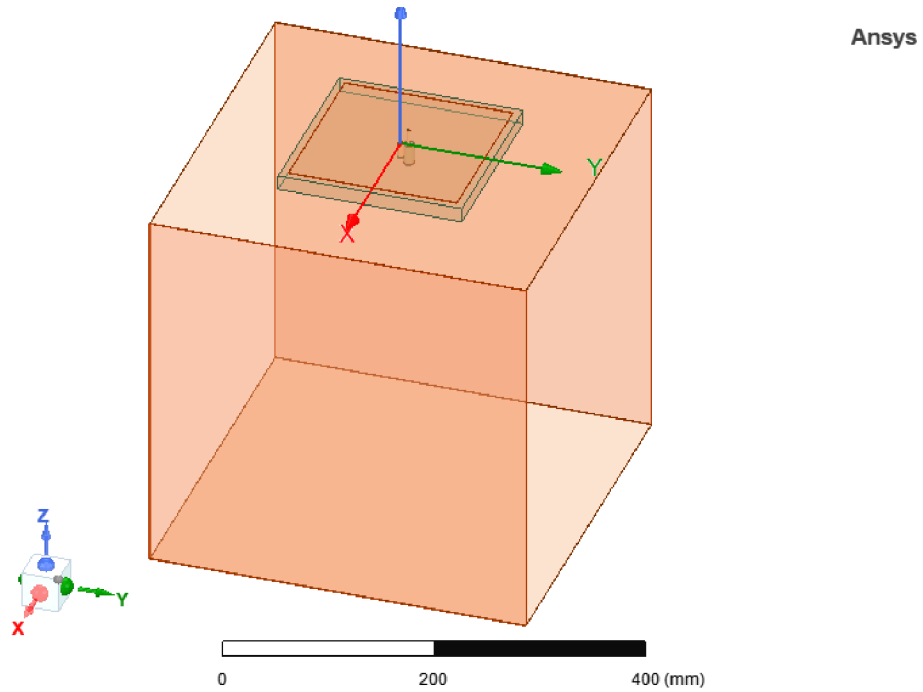


Fig. 3.13: Model of the antenna for main directions test

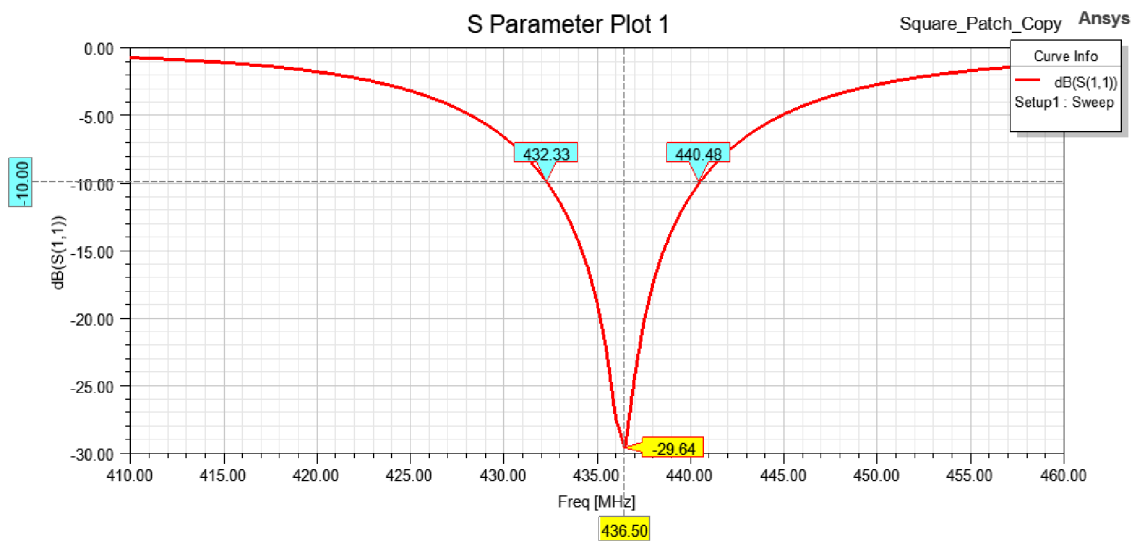


Fig. 3.14: Reflection coefficient s_{11} - cardinal directions test

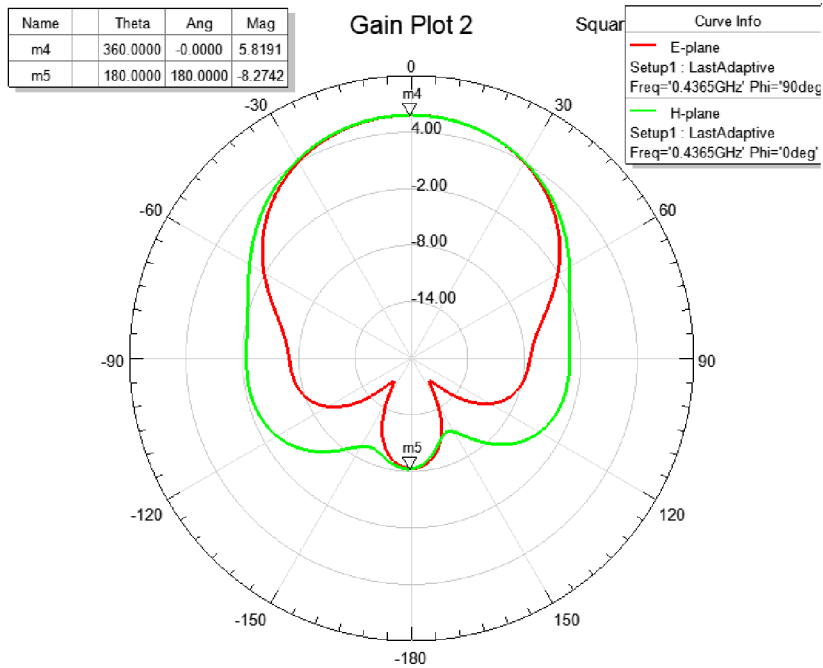


Fig. 3.15: Radiation pattern - cardinal directions test

Now that the antenna is designed, measured and verified in the simulator, the next step is design the antenna array with similar steps as with the single antenna design.

4. ANTENNA ARRAY

After verifying the single antenna design, the antenna is ready to be part of the antenna array. For this particular array, there are some conditions that must be met. Number of elements in the antenna array should be even, and not odd. With odd number of elements, antenna feeding would get more complicated. Also, since this is supposed to be a compact antenna design, the antenna array mustn't be too big. Hence, the antenna array consists of 2 elements. The goals for this design are achieving highest gain possible with only 2 elements while keeping side lobes and back lobes attenuated and keeping the array dimensions in compact size.

4.1 Array design

As mentioned above, the antenna array consists of 2 elements. This approach opens up 2 possibilities for the antenna tuning without worrying about dimensions too much. Since the single antenna is prepared, all that's left is copy the single antenna and place it next to it. As for antenna tuning, it's possible to increase or decrease antenna's gain (change in radiation pattern) or reflection coefficient by shifting antenna substrate position along x or y axis (depends on second antenna placement) symmetrically. In this case, the array is shifted along x-axis. The current developed in both antenna array elements depends on their own excitation and contributions from neighboring array element as well. This forms electromagnetic interaction between the antenna elements, also called as mutual coupling in antenna array [18]. The mutual coupling changes the radiation resistances of the coupled elements, which can lead to increased gain of the antenna array at the cost of increased side lobes [19]. The reason behind the position shifting of the array elements is the potential overlapping of the electrical fields, radiated by antenna elements. Shifting them way too close to each other will cause overlapping of the electrical fields, which will result in decrease of gain. By shifting their positions way too away from each other, the electrical fields will be too distant, which will result in increase of side lobes and decrease of gain as well, but only slightly. Hence, the best position is where the fields are nearly touching. A simple field layout of the array elements can be seen in Figure 4.1.

Another method is a simple extension of the ground plane, but only in one direction. In this case, it's along x-axis. By applying the ground extension, an extra distance for mutual coupling can be achieved. Again, expanding must be symmetrical as well.

The tuned antenna array with both methods applied is displayed in Figure 4.2. Combining those methods can boost the desired gain almost by 0.5dB. Of course, by tuning the antenna array incorrectly, the effect might be opposite and gain might be similar to the single antenna.

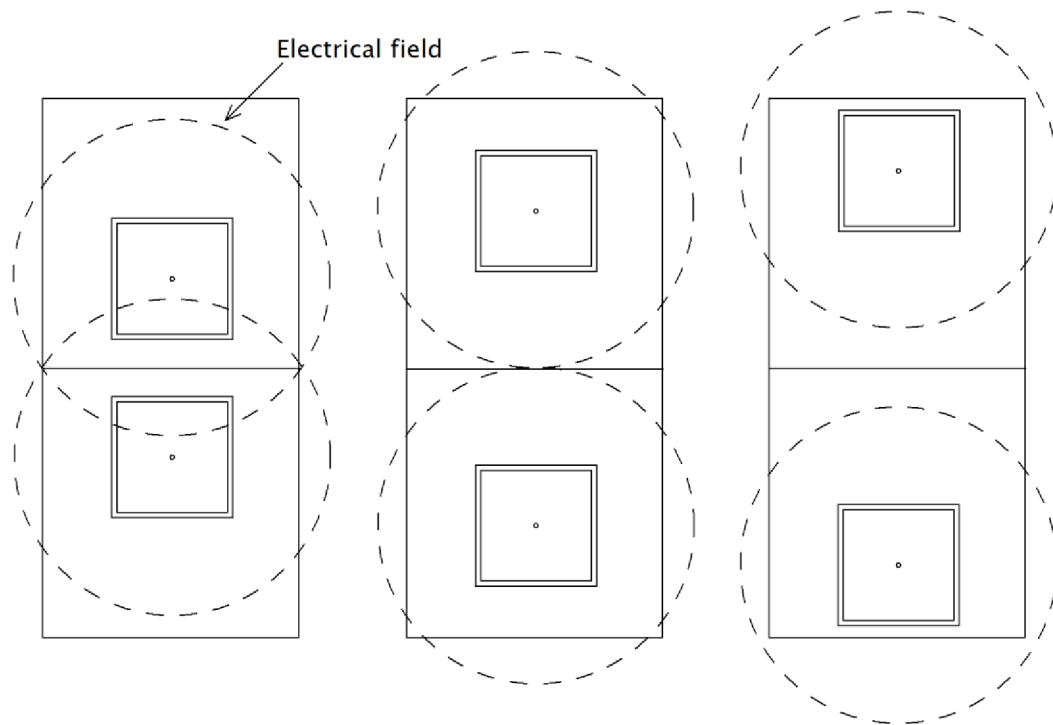


Fig. 4.1: a) Antenna array with overlapping E-fields (left), b) touching E-fields (middle) and c) distant E-fields (right)

Ansys

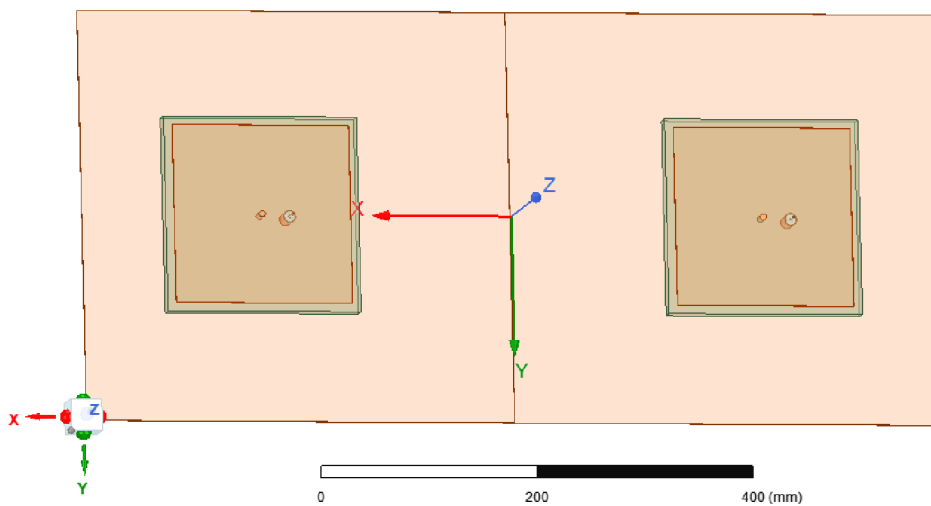


Fig. 4.2: Model of the tuned antenna array

For this antenna array, both tuning methods are applied. First of all, ground planes are expanded for both antennas by 20mm in x-axis. Overall, dimensions of the ground plane for the antenna array is 820x390mm. After expanding the ground plane, positions of the array's substrates are altered only in x-axis. Since the substrate placement is mirrored, position of substrates can be changed easily. New found position is +45mm from the antenna's initial position. It's important to keep things in order since

its meaningless shifting substrate before expanding the ground planes. Also, its meaningless expanding ground planes, in this case, in y-axis since substrates are shifted only in x-axis.

4.1.1 Feeding methods

There are two acceptable methods to go with, and those are connection of antennas with microstrips or connection with coaxial cables. Connecting the array elements with pieces of microstrip lines requires designing length of microstrip lines with required impedance as well. Since this method is a little bit complicated, the best method is connecting array elements with 50Ω coaxial cables.

Using coaxial cables can save extra work and time mainly because all there must be done is to follow the design scheme in Figure 4.3. The chosen coaxial cable for connecting the array elements is RG316, a flexible single shielded coaxial cable, capable to operate up to 3GHz with characteristic impedance 50Ω . It's primarily used for communication systems and antenna feeds, which makes it a perfect choice [20].

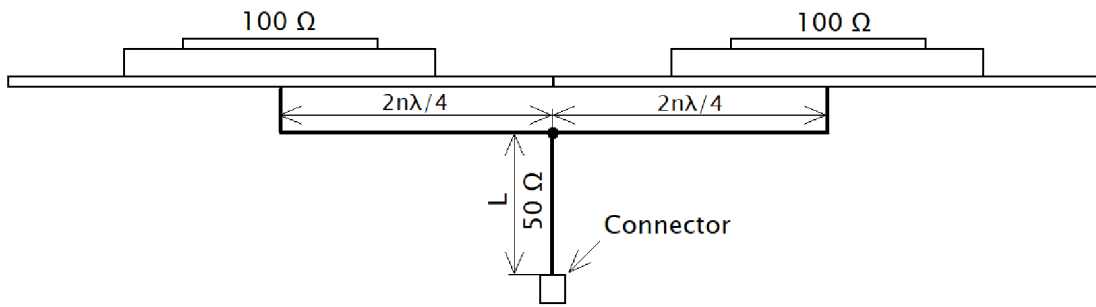


Fig. 4.3: Initial scheme of array cable feeding

Now that the feeding method of array elements together with proper cables are chosen, all that's left is to choose and calculate length of coaxial cables. The pair of coaxial cables are $2n\lambda/4$ long and so, their length must be calculated. The parameter n characterizes the number of rotations around the Smith diagram, where $n = 1$ means a full rotation. At first glance, the length calculation doesn't seem to be very difficult, but the key lies in the parameter k , which is located in wavelength λ . Their relation is shown in (4.1). The parameter k is the velocity factor or velocity of propagation, which is defined by the ratio of the mechanical length l of the transmission [21]. In this case, the velocity factor k for coaxial cable RG316 is 69% or 0.69 [20]. Velocity factor can be calculated by using formula in (4.1), but since the velocity factor is already known and what is needed is the physical length of coaxial cable l_f , the formula (4.1) must be modified.

$$k_0 = \frac{l_f}{l_e} = \frac{4 \cdot l_f}{2 \cdot n \cdot \lambda_0} \quad 4.1$$

The desired physical length l_f of coaxial cable can be calculated by using (4.2), where l_e is electrical length of coaxial cable [20].

$$l_f = \frac{k \cdot n \cdot \lambda_0}{2} = \frac{0.69 \cdot 1 \cdot 0.687}{2} = 240\text{mm} \quad 4.2$$

A new found length of coaxial cable is 240mm. Now the important thing is to find out if the found length is suitable. Overall dimensions are displayed in Figure 4.4. The total width of the array is 820mm, the left array element feed is 55.3mm far from the edge of patch. A space between patch and substrate is 8mm wide and the distance between 2 array elements is 295mm. The right element feed is 113.7mm far from the edge of patch. Including another gap between patch and substrate, that makes a total of 480mm between left and right array element feed, which is exactly the found length of both coaxial cables, hence $2 \times 240\text{mm}$ is 480mm. If the calculated length would be greater than 240mm, then another length must be calculated using parameter $n > 1$. Since the calculated length is similar to length between coaxial probes, instead of common connector for both RG316, there is another RG316 between them with arbitrary length L . At the end of this coaxial cable is connected a SMA connector.

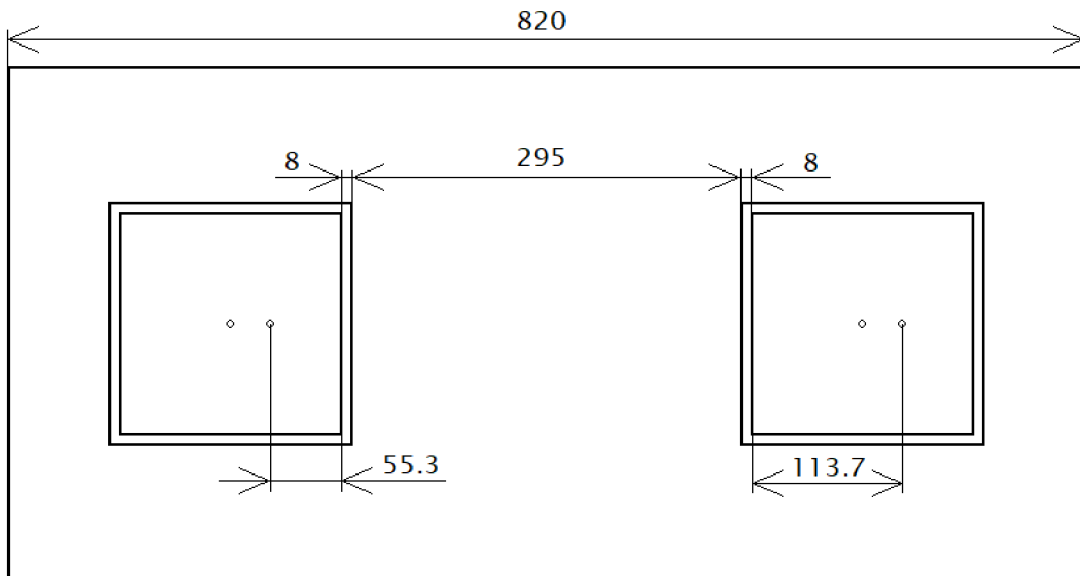


Fig. 4.4: Distance between array element feeds

4.1.2 Miscellaneous changes

Since copper is used in real world less frequently and is more expensive, instead of copper, aluminum is used for antenna patches and ground plane. The material itself won't have a huge impact on the results of the antenna array, but the catch is that the

aluminum is commonly produced with thickness 1.5mm. This may have a small impact on the results like resonant frequency shifting.

Another change to the antenna array are holes made into every corner of the patch, 4 holes in total with radius of 2mm for each array element 5mm away from the edges of the patch. These holes are going through the patch, all the way through substrate and ground plane. These holes are for plastic screws, which will keep the whole antenna in one place. The plastic screws have more or less the same relative permittivity as the substrate. That's why in the simulator the holes are filled with the dielectric substrate as a substitution for the plastic screws, meaning holes in the patch and the ground plane are filled Ertalon as well. The applied changes are shown in Figure 4.5. This change may have an impact on the results as well like previously mentioned resonant frequency shifting or increase in reflection coefficients s_{11} and s_{22} . In chapter 4.2 – Reflection coefficient, are described differences and impacts of applied changes on antenna array.

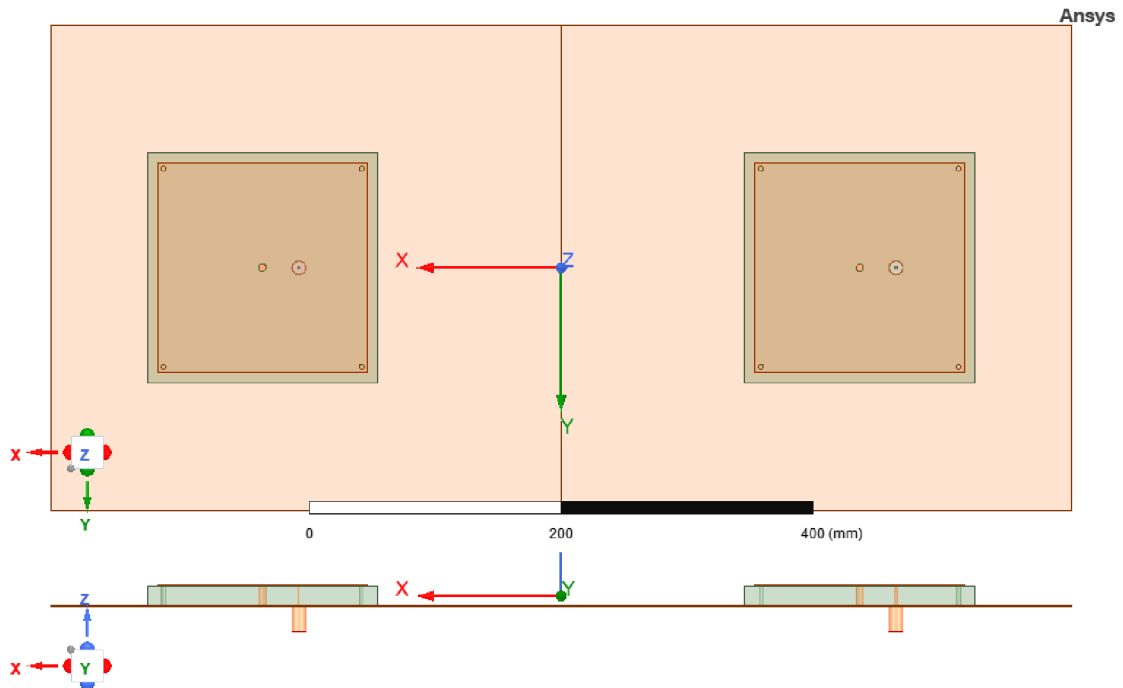


Fig. 4.5: Antenna array model with applied changes

4.2 Reflection coefficient

The reflection coefficient is simulated with and without previously mentioned changes. Although the position of coaxial feed has been determined (39.7mm), the reflection coefficient is way too high, thus the coaxial feed needs to be slightly altered. Also since there are two array elements, then there are two coaxial feeds as well, hence two reflection coefficients s_{11} and s_{22} are simulated simultaneously. The simulated reflection coefficients s_{11} and s_{22} with and without mentioned changes are shown in Figure 4.6 and

4.7. By leaving the antenna array without thickness adjustment and holes, the value of reflection coefficients are, with new found coaxial feed position 29.2mm $s_{11} = -51.76\text{dB}$ and $s_{22} = -47.16\text{dB}$. The resonant frequency shifted from desired 436.5MHz to 436.88MHz. The shift in resonant frequency isn't that huge, and so it can be neglected. Now with added drill holes and thickness of the patch and the ground plane, the value of reflection coefficients on desired resonant frequency 436.5MHz is $s_{11} = -35.29\text{dB}$ and $s_{22} = -34.99\text{dB}$, which is higher than before. But this time, no frequency shifting has occurred.

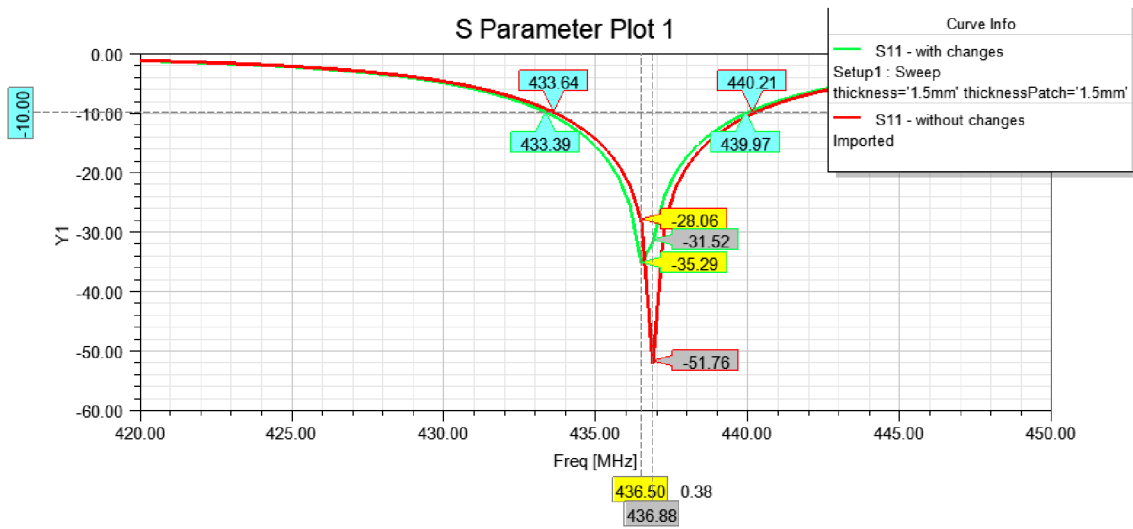


Fig. 4.6: Reflection coefficients s_{11} with and without applied changes

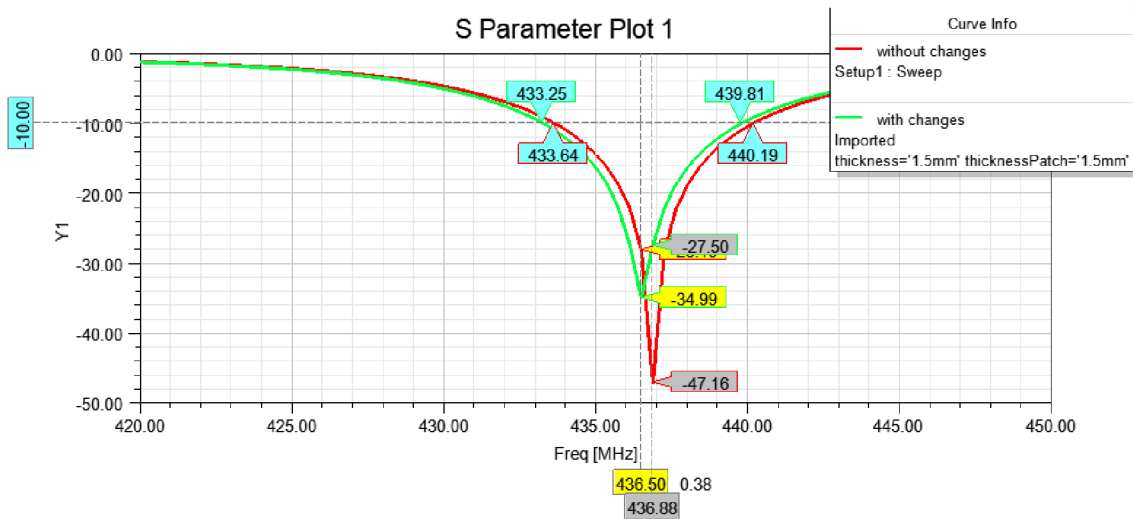


Fig. 4.7: Reflection coefficients s_{22} with and without applied changes

4.3 Radiation pattern

The radiation pattern of the single antenna is too wide, its gain is too low for intended uses and it has fixed radiation pattern aiming [23]. Now with the designed model of 2-element antenna array, the radiation pattern looks a bit different. The main lobe is much narrower, the side lobes are growing and nulls are created between a side lobes and main lobe. Null is observed in directions, where the waves, from side lobes and main lobe (or side lobes and back lobe), add destructively, thus resulting in minima of the radiation. To put it more simply, it adds an empty space between side lobes and main lobe (or back lobe). On the other hand, in directions where the waves are added constructively are maxima of the radiation, for example main lobe [23]. Figure 4.8 explains closer a creation of constructive and destructive waves.

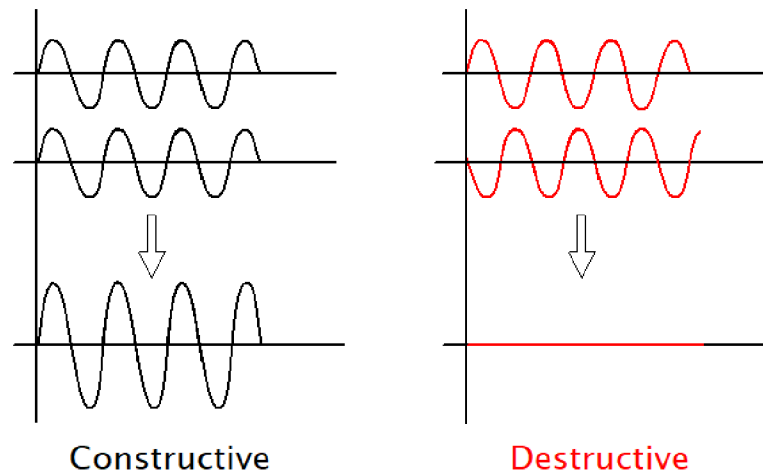


Fig. 4.8: Creation of constructive and destructive waves

Figure 4.9 shows the radiation pattern of 2-element antenna array without tuning with intentionally moved array elements far from each other, precisely 90mm from the origin or 385mm from each other (similarly in figure 4.1 – a)). The first thing to notice is growth of the side lobes and back lobe. The values of side lobes significantly increased and the value of back lobe is positive, meaning it's no longer attenuated. The nulls in radiation pattern are widening as well and the gain in main lobe decreased by approximately 0.25dB.

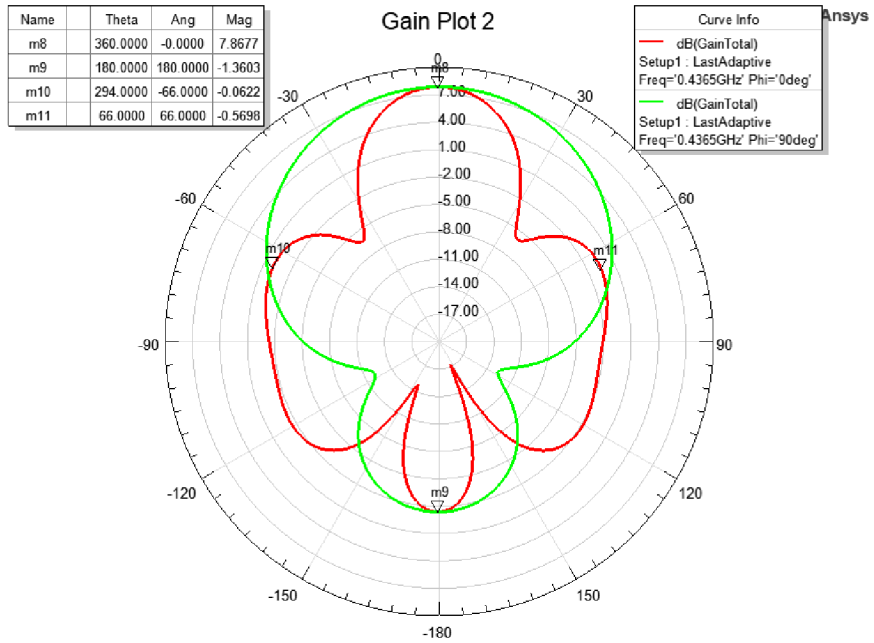


Fig. 4.9: Radiation pattern of the 2-element array without tuning (distant elements)

Figure 4.10 shows the radiation pattern of 2-element antenna array without tuning with intentionally moved array elements too close, precisely 45mm from each other (similarly in Figure 4.1 – c)). The nulls and side lobes disappeared and the back lobe is miniscule. The total gain significantly decreased to value 7.09dB, which is almost a 0.8dB difference compared to the model with distant elements.

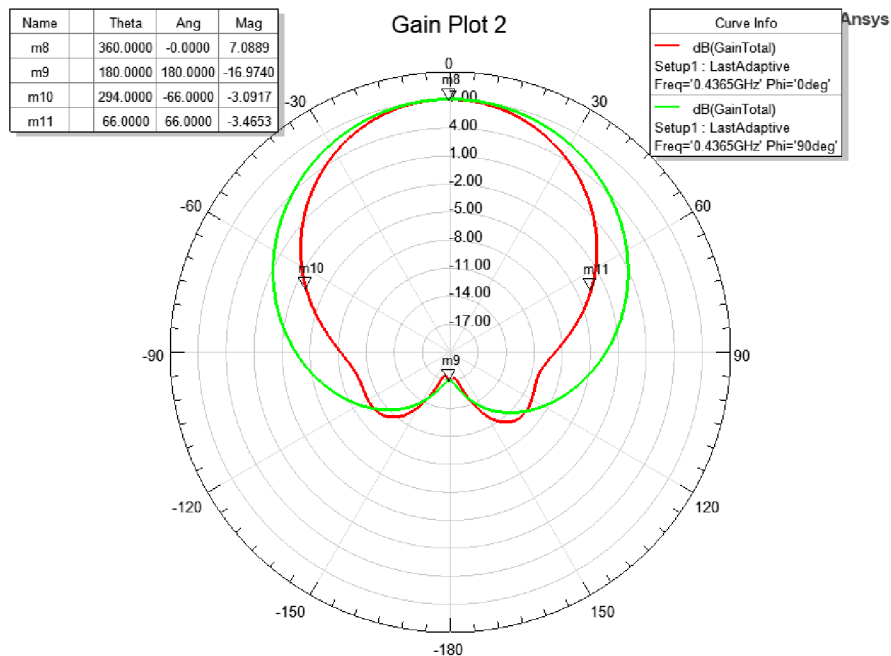


Fig. 4.10: Radiation pattern of the 2-element array without tuning (close elements)

The main goal is to keep side lobes and back lobe attenuated while keeping the main lobe with as much gain as possible. The total gain of the antenna array is 8.1dB. The radiation pattern of the tuned antenna array is shown in Figure 4.11 and Figure 4.12 shows the 3D radiation pattern of the tuned antenna array.

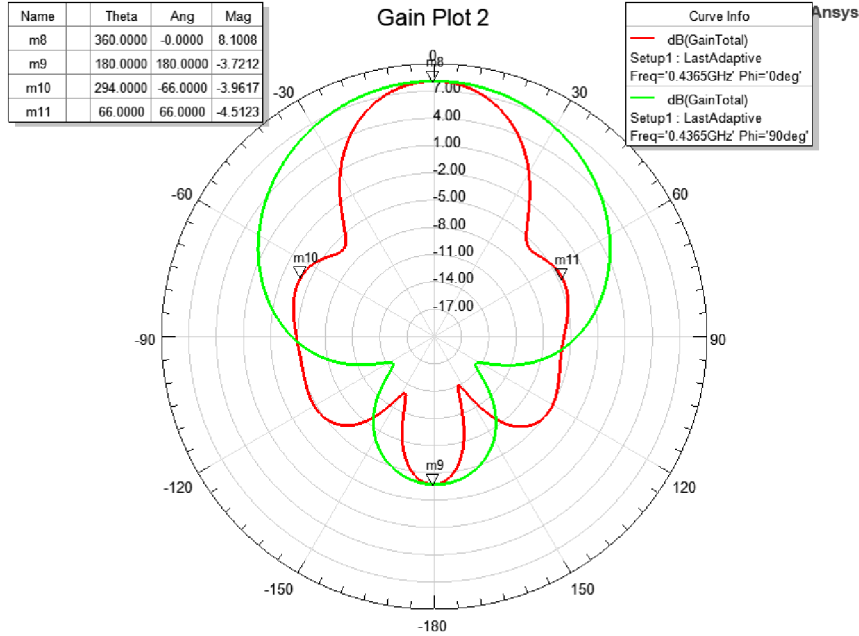


Fig. 4.11: Radiation pattern of the tuned 2-element array

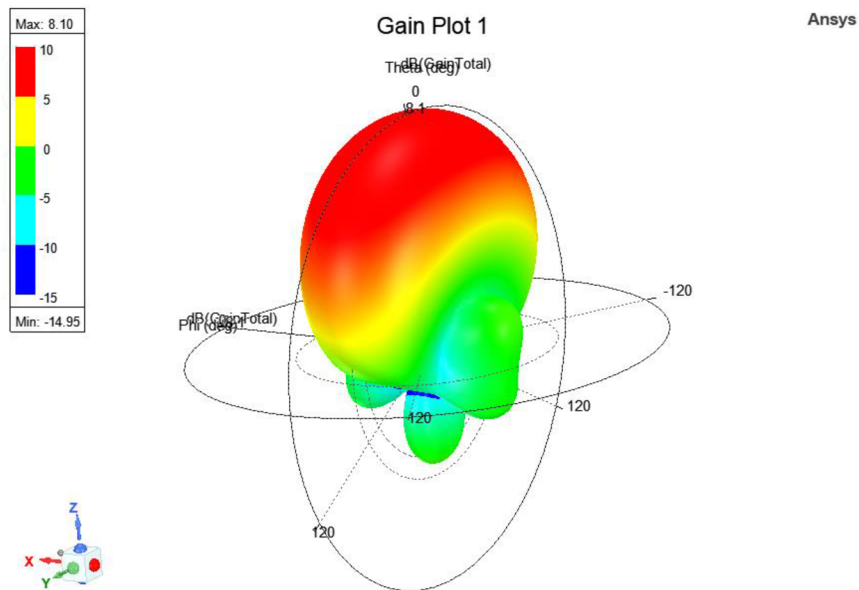


Fig. 4.12: 3D radiation pattern of the tuned 2-element array

4.4 Comparison between two and three-element array

With another element added to the antenna array, the 3-element antenna array is created. Its model is displayed in Figure 4.13. One thing to mention regarding the antenna array

tuning is, expansion of the ground plane along x-axis can be used to squeeze out a little bit of gain from the antenna array, but shifting the array elements along the x-axis like with the 2-element array can't be used due to its asymmetry. Same goes for the feeding method used in the 2-element array. That's why both the 2-element array and 3-element array are compared with each other with both array elements in their initial position and without any adjustments to dimensions.

Ansys

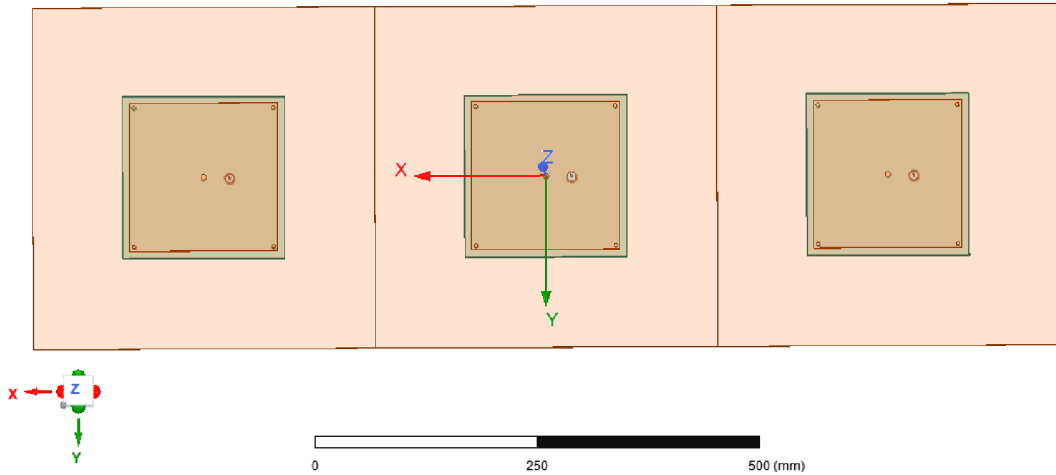


Fig. 4.13: Model of 3-element antenna array

Reflection coefficients of 3-element array for all 3 ports are almost the same. Comparing the reflection coefficient s_{11} to the 2-element model s_{11} , their shape is similar and their value differ by approximately -4dB. Reflection coefficients of both antenna arrays are displayed in Figure 4.14, with only 1 port s_{11} from 2-element array as comparison.

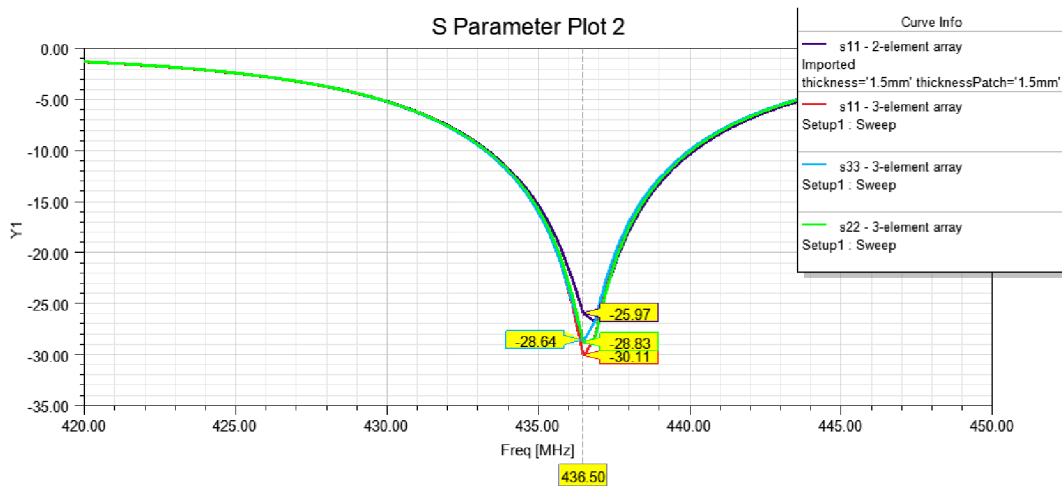


Fig. 4.14: Reflection coefficient of 3-element and 2-element antenna array

Like mentioned before in chapter 4.1, by adding another element into the array, its gain will increase and its main lobe will get narrower [23]. Figure 4.15 shows

differences in radiation pattern between 2-element and 3-element array. In this case, the back lobe is higher, the side lobes got significantly bigger and nulls are much deeper than in 2-element array model. But even without shifting the array elements or extending the ground plane, the total gain of 3-element array is much higher than the total gain of 2-element array. Figure 4.16 shows 3D radiation pattern of the 3-element antenna array.

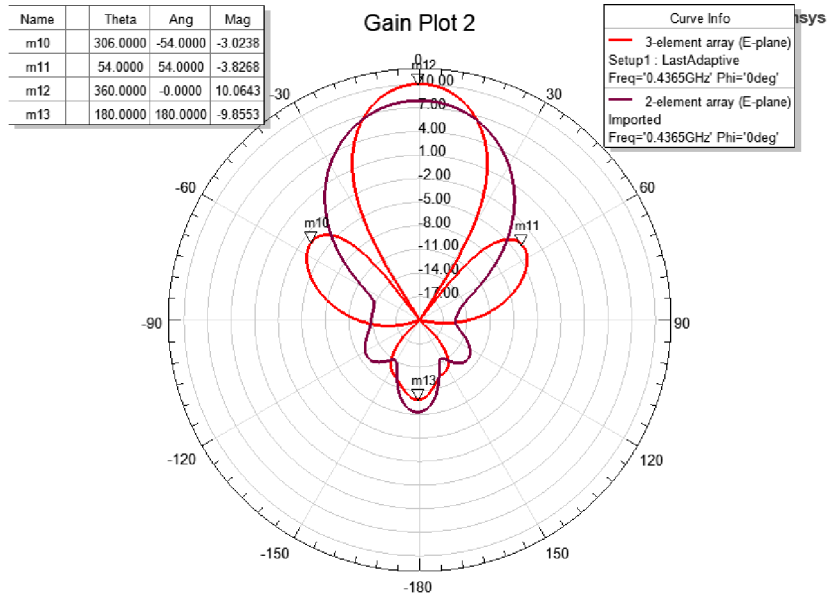


Fig. 4.15: Radiation pattern of 3-element and 2-element antenna array

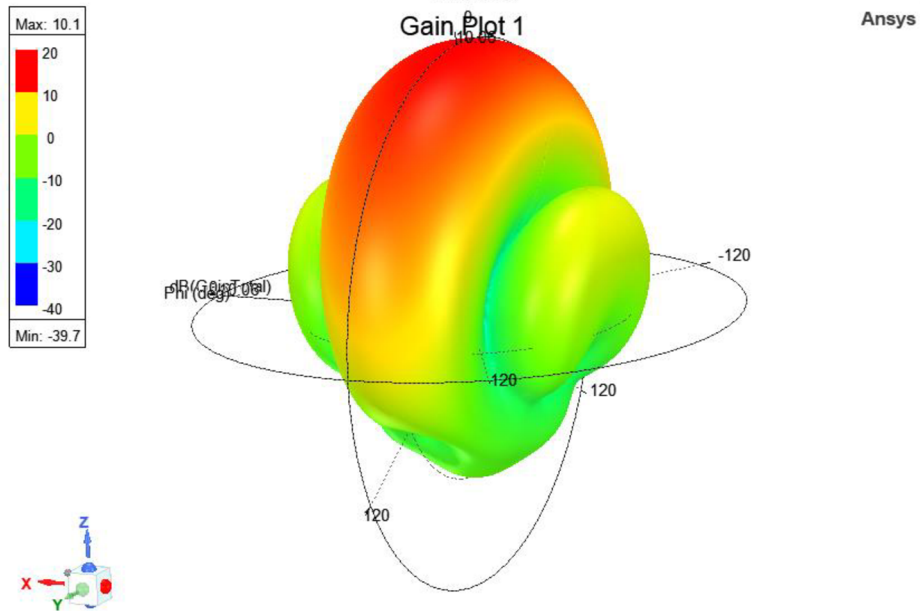


Fig. 4.16: 3D Radiation pattern of 3-element antenna array

Even though the 3-element array seem like a better choice, mainly because of the total gain in radiation pattern, the complexity of the design, its feeding method, odd

number of array elements and overall size of the antenna array makes it less favorable to produce.

4.5 Verification of the antenna array

Similarly as with the single antenna, the design of 2-element antenna array is verified with the same methods, but now for both array elements instead of one.

By adding additional coaxial probe with the same offset from the middle as the original one, it's possible to verify functionality of the design. If the reflection coefficients s_{11} and s_{33} (1st element) or s_{22} and s_{44} (2nd element) are same or similar without any shifts in resonant frequency, the design works as intended. Figure 4.17 shows the model with additional coaxial probes and Figure 4.18 shows the reflection coefficients. The shape and values of reflection coefficients s_{11} and s_{33} are similar, while the shape and values of reflection coefficients s_{22} and s_{44} differ a little bit. The reflection coefficients for both elements changed in values approximately by +4dB from the original. The resonant frequency changed to 436.9MHz, with only 0.4MHz difference, which can be neglected. To sum things up, the design is so far stable.

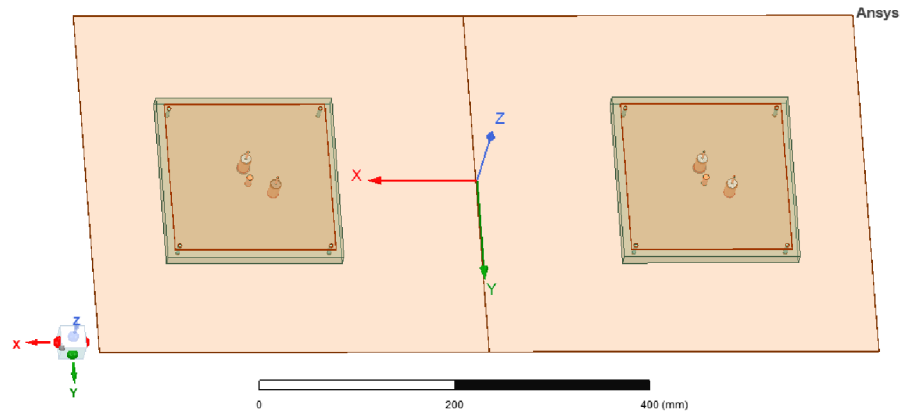


Fig. 4.17: Model of 2-element array with additional coaxial probes

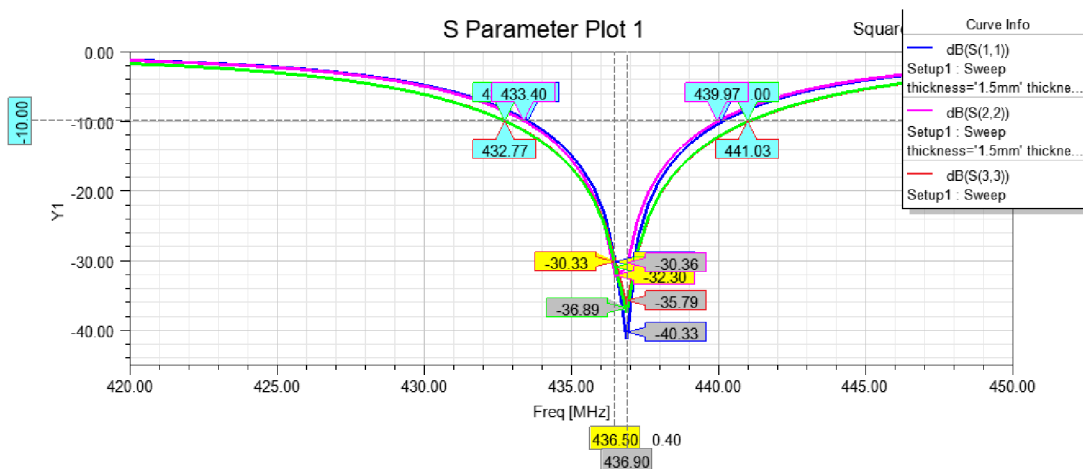


Fig. 4.18: Reflection coefficients of 2-element array – functionality test

Similarly as in chapter 3.5, by adding ground planes along x-axis in rectangular formation, it's possible to simulate a behavior of the antenna array in case of radiation in all 4 cardinal directions. Figure 4.19 shows the modified model, while Figure 4.20 and Figure 4.21 shows the reflection coefficients and the radiation pattern.

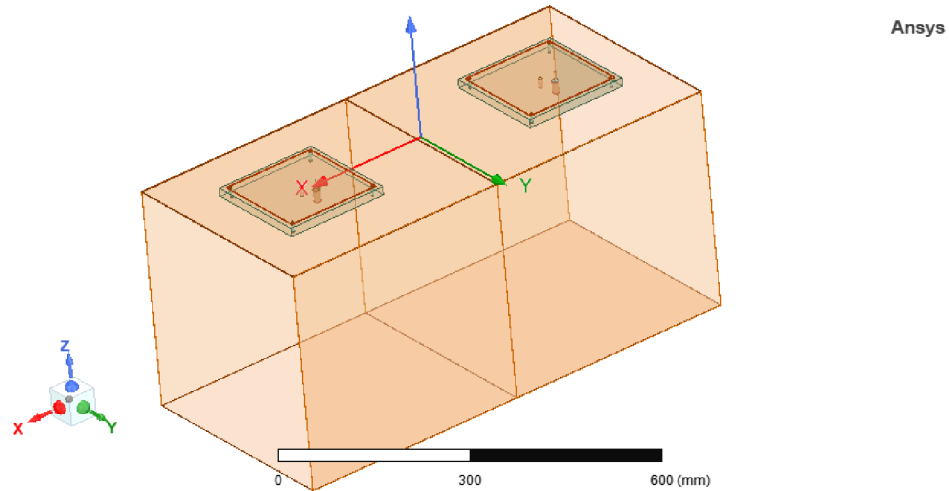


Fig. 4.19: Model of the antenna array for cardinal directions test

The resonant frequency in Figure 4.20 didn't move at all, in fact the value of reflection coefficient s_{11} show an approximate -3dB improvement compared to the original, while reflection coefficient s_{22} got worse by approximately +3dB.

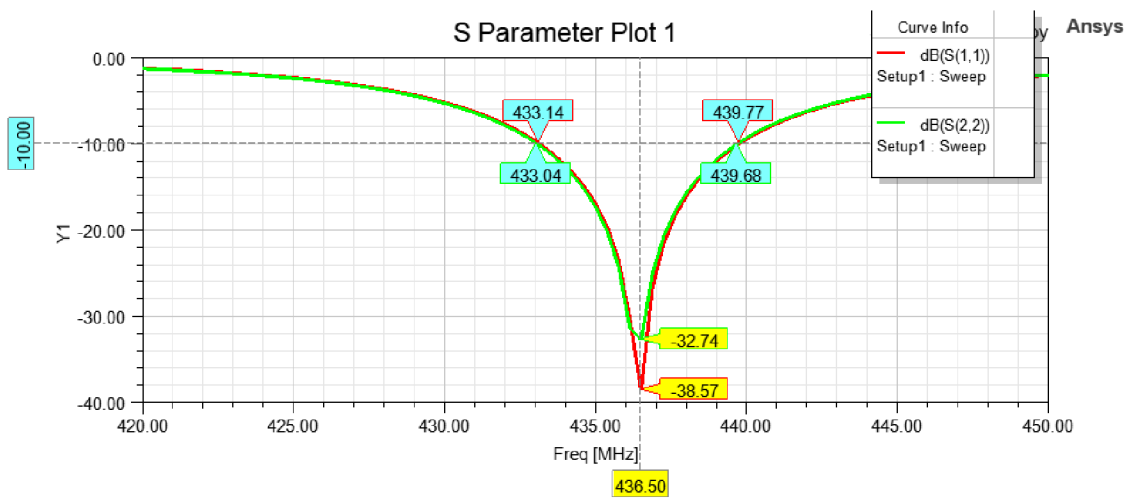


Fig. 4.20: Reflection coefficients s_{11} and s_{22} - cardinal directions test

As for the radiation pattern, the total gain increased by approximately 0.3dB, which is an improvement. Side lobes and back lobe have increased bit more than in the original, but they still remain attenuated.

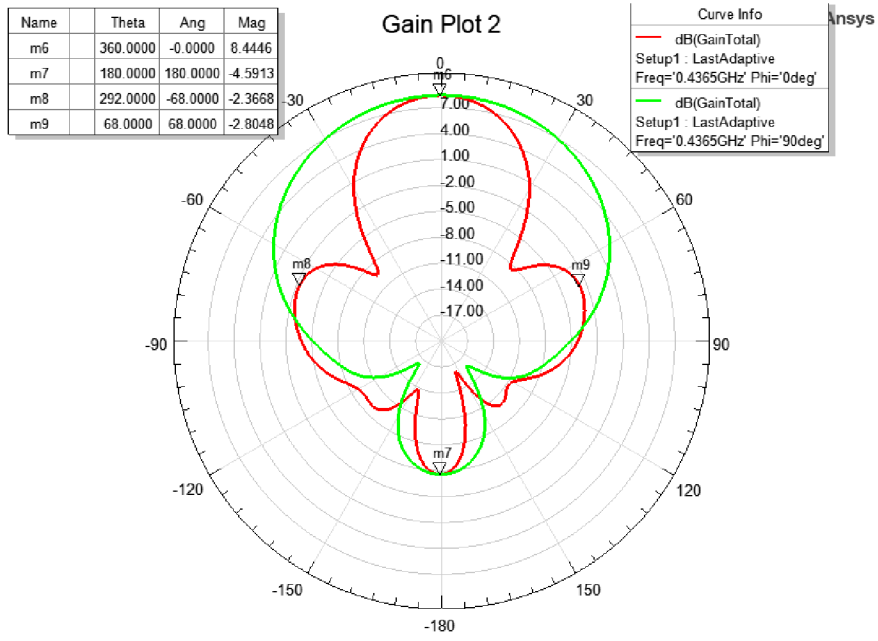


Fig. 4.21: Radiation pattern - cardinal directions test

5. ANTENNA BUILDING AND TESTING

With the designed and simulated antenna array model, the physical model can be produced and measured. But first, the single antenna model is produced and tested. The reason behind it is to measure and check functionality of the initial design, find potential errors in the physical model and compare simulated data with measured data. Once everything is measured and confirmed in the single antenna model, the antenna array can be produced. There are two options to measure and check functionality of the antenna array model. The first one is to physically make and build the antenna array like the first single antenna. The second option is to convert the antenna array model from the simulator to .sat file. This file serves to store 3D geometry information within a standard text format and is used to exchange 3D data between multiple systems. It's usually used in computer-aided engineering, shipbuilding, 3D animation, etc. [24].

5.1 Building and testing the single antenna

As mentioned before, the single antenna is physically produced as well. Its main purpose is to compare measured data with simulated results. If measured data, in this case reflection coefficient, corresponds with simulated results, then the antenna works as intended. Figure 5.1 shows the section view of the single antenna.

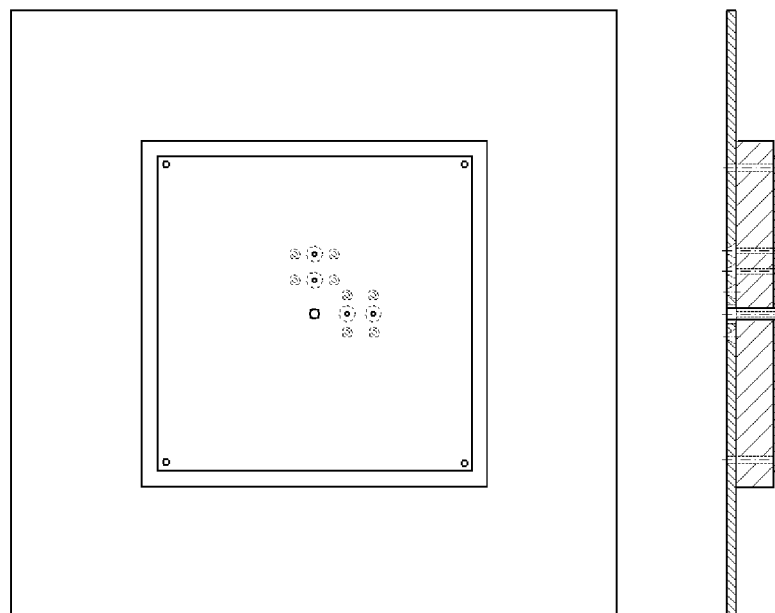


Fig. 5.1: Top and side section view of the single antenna

The single antenna consists of 2 aluminum squares (patch and ground) and dielectric substrate made out of Ertalon. Since Ertalon is a little bit slippery, a 4 plastic screws are

used to secure the whole antenna in one place. The middle screw serves as pin, connecting the patch and ground plane. To check proper functionality and stability of the single antenna, the model with 2 coaxial probe is used. Also to see, if the single antenna works with 50Ω , 2 holes for coaxial feed are added with diameter 3mm. Between a coaxial probe are added 2 holes for additional screw. Those screws serve for connecting outer conductor (shield) to the antenna. As a probe, a screw with diameter 3mm is used going through the patch, all the way through the substrate to the ground plane. Figure 5.2 show a board of patch, made in Autodesk Eagle. This is an example of how dimensions for the antenna and holes are drawn for manufacturing. Red outlines serve as information, meanwhile vias (green circles) serve as place for holes. The boards with the dielectric substrate and the ground plane with corresponding dimensions and holes placement are drawn as well.

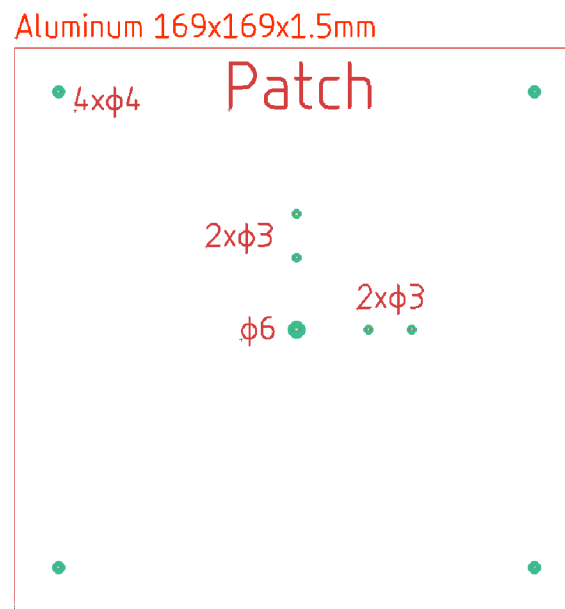


Fig. 5.2: Example of drawn patch board

Figure 5.3 shows fully build antenna from top and bottom view. Now with built model, a measurement can be conducted. Since the antenna is meant to be for 100Ω , measurement for 100Ω is conducted first. Firstly, the reflection coefficient is measured. Figure 5.4 shows a comparison between simulated result (100Ω port) and newly acquired data from measurement (50Ω port) of the 100Ω antenna. The measured results are terrible. The resonant frequency of the build antenna lies on 488.75MHz , which is a 52.25MHz difference. The value of measured reflection coefficient dropped to -13.38dB , which is a huge difference from the simulated. By checking smith chart on the vector network analyzer, the impedance of the antenna dropped to approximately 70Ω (real) and $j30\Omega$ (imaginary). By switching to the 50Ω antenna, the results are showing similar frequency shifting and even lower reflection coefficient.



Fig. 5.3: The fully build single antenna (top view)

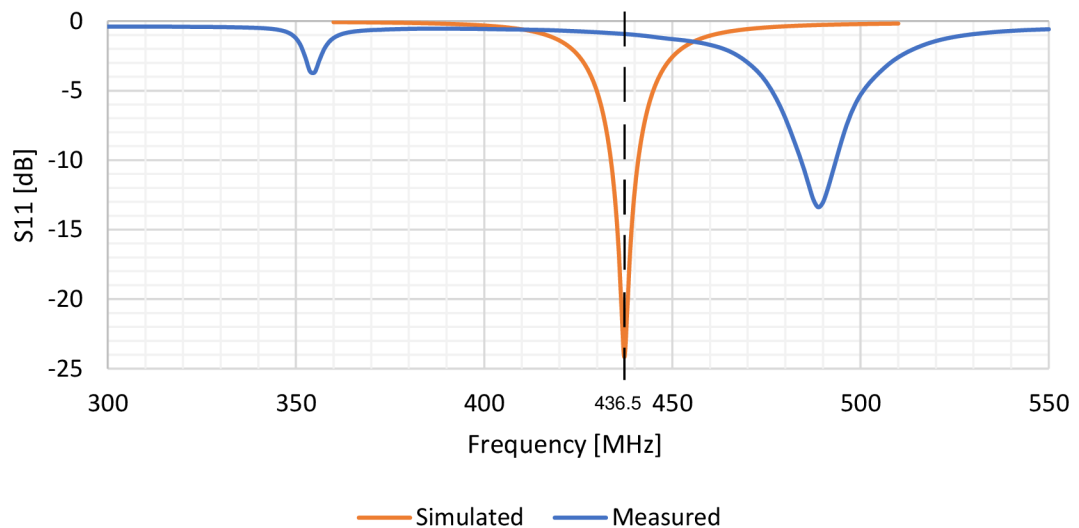


Fig. 5.4: Measured and simulated reflection coefficient (100Ω)

5.1.1 Troubleshooting

The cause of this problem might be a change of relative permittivity in the dielectric substrate. By working with higher frequencies, which are hundreds of MHz, the relative permittivity loses its value. This means, a new real relative permittivity must be found. This can be accomplished by using the measured data of the reflection coefficient and simulated model of the single antenna in the simulator. By slowly lowering relative permittivity of the simulated dielectric substrate, the simulated reflection coefficient is shifting toward the frequency 488.75MHz. Once the simulated reflection coefficient is matched with the measured one or their resonant frequencies are the same or similar, the real relative permittivity is found. In this case, the found relative permittivity is $\epsilon_r = 2.97$.

Another problem that can be seen from Figure 5.4 is much smaller reflection coefficient of the measured antenna, which means the impedance of the antenna is much smaller as well. This might have been caused by increased dielectric tangent loss. By increasing the value of the dielectric tangent loss, the impedance of the antenna is decreasing. The true value of dielectric tangent loss can be found by matching the measured impedance of the antenna to the simulated one. The found value of the dielectric tangent loss is 0.1. With newly found information, the single antenna can be rebuilt.

5.1.2 Redesigning, Rebuilding and testing

By finding the real relative permittivity $\epsilon_r = 2.97$ and real dielectric tangent loss $\tan\delta = 0.1$, the single antenna can be designed and tuned from the start once again. By increasing the dimensions of the patch, the resonant frequency is shifting towards the desired/required one. Final dimension of the patch is 188mm, which is 3mm wider than dielectric substrate. That means the dielectric substrate must be wider as well. This time, the substrate is intentionally much wider than patch. Its final dimension is 216mm. The ground plane stays as it is, since making it wider would lead to unnecessary growth in dimensions of the antenna array. The new found position of the coaxial probe for the 50 Ω placement is approximately 50mm from the middle of the antenna and for the 100 Ω , the new found position of the coaxial probe is approximately 90mm from the middle of the antenna.

Simulating the new model of single antenna is the same as before. This time, the antenna model with 2 coaxial probes is simulated to save time. One probe is set to 50 Ω , 50mm from the middle of the antenna and the second probe is set to 100 Ω , 90mm from the middle of the antenna. Figure 5.5 shows the simulated reflection coefficient of s_{11} and measured s_{11} for 50 Ω antenna, while Figure 5.6 shows the simulated reflection coefficient of s_{22} and measured s_{22} for 100 Ω .

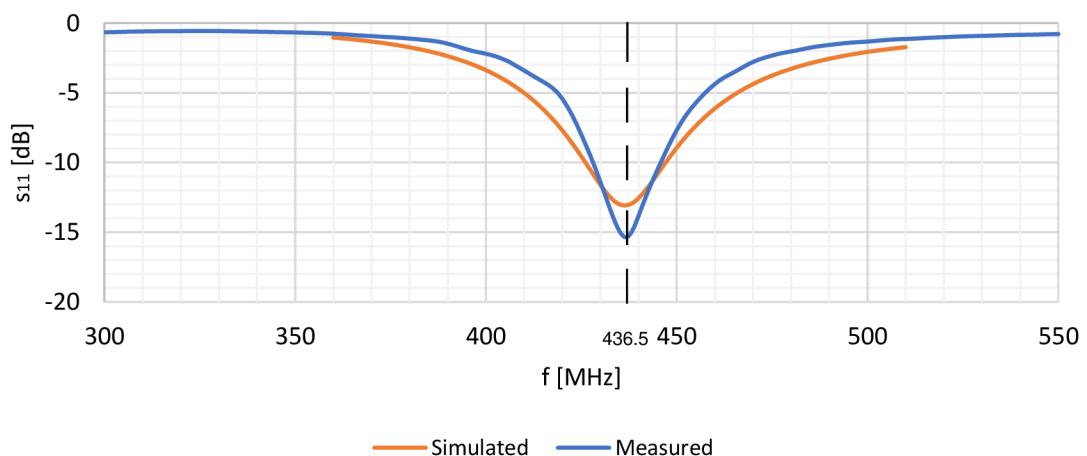


Fig. 5.5: Comparison between simulated and measured s_{11} of the new antenna (50 Ω)

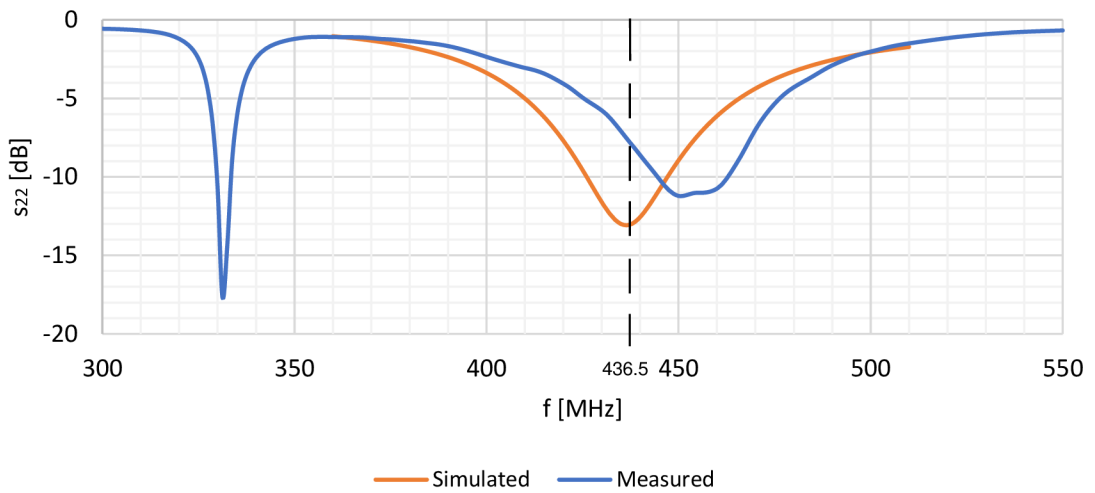


Fig. 5.6: Comparison between simulated and measured s_{22} of the new antenna (100Ω)

Secondly, the radiation pattern of the newly created antenna model is created, shown in Figure 5.7, the shape itself is almost the same as in the previous model, but the gain significantly decreased to value 1.5dB, which makes the single antenna unusable.

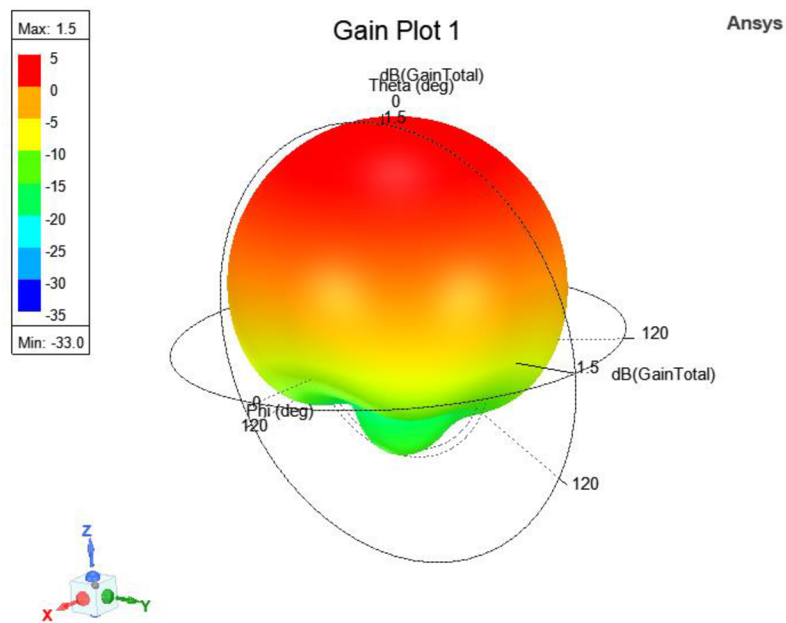


Fig. 5.7: 3D Radiation pattern of the newly created antenna

5.2 Verification through .sat file

Since it wasn't possible to measure the radiation pattern physically, thanks to doc. Ing. Jaroslav Lačík, Ph.D., the single antenna design has been verified numerically in

another simulator CST microwave studio, using .sat file from HFSS Ansys. In Figure 5.8, the verified reflection coefficient (50Ω) shows similarities to the simulated one. Resonant frequency of the verified one is slightly shifted to value 444MHz and its reflection coefficient is slightly lower with value of -14.52dB.

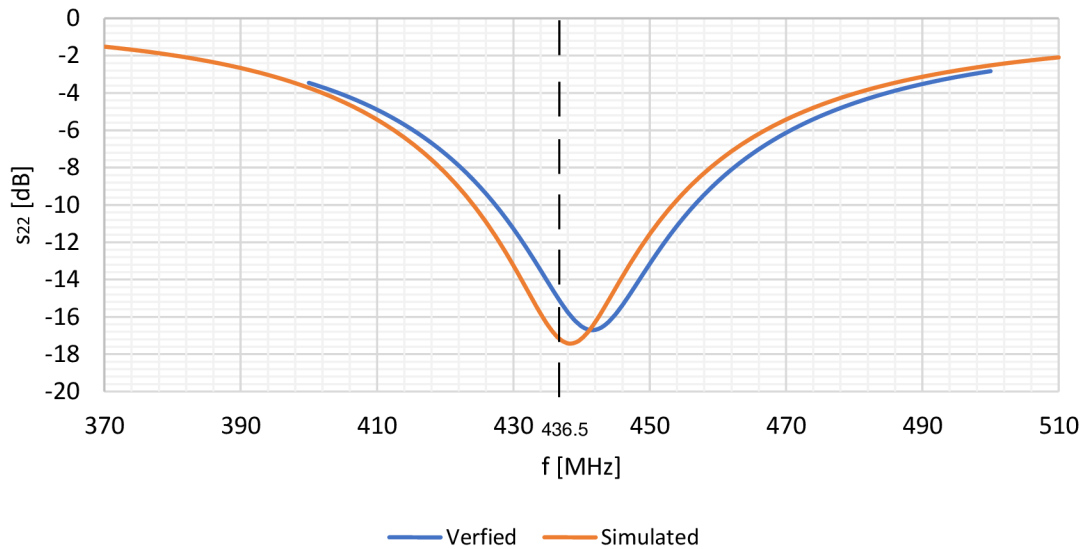


Fig. 5.8: Comparison between verified and simulated reflection coefficient (50Ω)

The verified reflection coefficient (100Ω) displayed in Figure 5.9, shows similarities to the simulated one as well. Resonant frequency of the verified one is slightly shifted to value 442MHz and its reflection coefficient is slightly lower with value of -16.7dB.

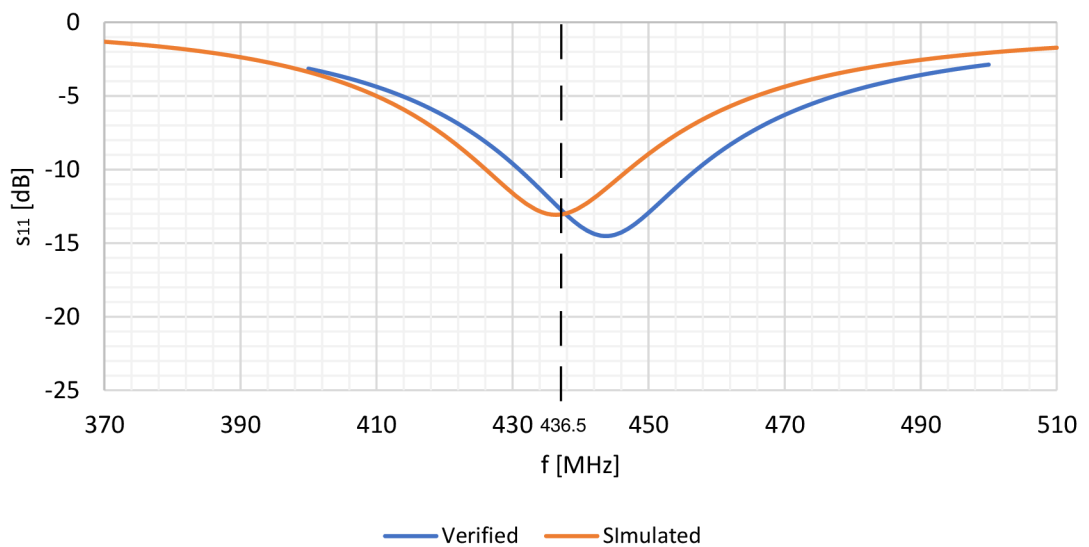


Fig. 5.9: Comparison between verified and simulated reflection coefficient (100Ω)

The verified radiation pattern is compared to the simulated one similar, but the value of total gain is 1.08dB, which is a 0.42dB difference from the simulated one. The verified radiation pattern, exported to HFSS Ansys, can be seen in Figure 5.10.

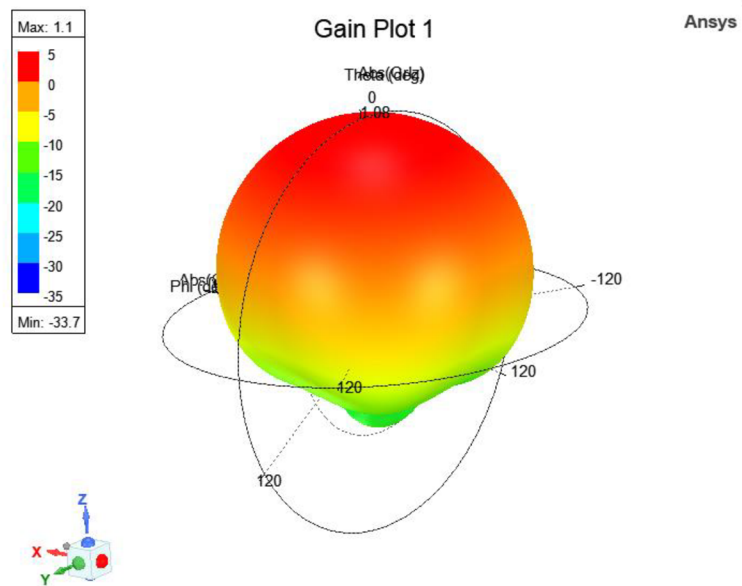


Fig. 5.10: 3D Radiation pattern of the verified antenna

6. CONCLUSION

The assignment was to make a statistical evaluation of the position of the satellite on a low orbit relative to the ground station, determine the possible benefits of coverage reductions and to create a model of a compact antenna array in the HFSS Ansys program with the reception of two linear polarizations perpendicular to each other, and implement, measure and verify the antenna.

In the first chapter, the data of elevation, azimuth, period and range between the BDSAT-2 satellite and the location of the ground station were obtained with the help of appropriate software. The data were obtained for two places, Brno and Longyearbyen, which were compared to each other. Subsequently, elevation and azimuth histograms were made for both locations with a 20% coverage reduction. Lastly, the potential gain of the antenna was calculated depending on the range and elevation of the satellite, based on the calculated gain and elevation angle, the ideal radiation pattern was made as a reference for choosing the right antenna.

The second chapter deals with the design of a single square patch antenna fed by a coaxial probe. The antenna is designed for a resonance frequency of 436.5MHz. First, a suitable substrate was chosen and its height from calculated range was determined. Subsequently, the dimensions of the square patch were calculated as accurately as possible, and the position of the coaxial probe from the center of the square patch was determined.

In the third chapter, the single antenna design was modeled in the HFSS Ansys program. The goal was to simulate the reflection coefficient, bandwidth, the antenna's resonant frequency and radiation pattern of the single antenna. The single antenna is resonating on 436.5MHz with bandwidth 7.84MHz (50Ω). The radiation pattern shows the gain of the antenna with value of 6.27dB with attenuated side lobes and back lobe. The single antenna design was verified by adding vertical and horizontal polarization, and another ground planes in square shape. The results are very similar to the previous results, the single antenna design works as intended.

In the fourth chapter, the 2-element antenna array is designed, based on the single antenna design with small adjustments to the patch and the ground plane thickness and holes, intended for plastic screws. This time, the antenna array was designed for 100Ω. Taken steps in designing the antenna array are similar as with the single antenna, but this time the tuning methods, like shifting substrate placement, were implemented for the maximum gain output. The 2-element antenna array is resonating on 436.5MHz with bandwidth on average 6.56MHz. The radiation pattern shows the gain of the antenna with value of 8.1dB with attenuated side lobes and back lobe. By the same means as the single antenna, the antenna array was verified. The results are very similar to the previous results as well, the single antenna design works as intended.

In the last chapter, the single antenna was build and measured first to verify the design itself and find any potential flaws. The measured reflection coefficient of the single antenna (100 Ω port) was a lot worse than expected. The main reason is the change of relative permittivity and dielectric tangent loss in the dielectric substrate, caused by working with higher frequencies, which are hundreds of MHz. That caused several changes in the antenna's behavior are the resonant frequency, impedance, value of reflection coefficient and gain. By measuring impedance and reflection antenna, the true substrate parameters were found. Based on the new parameters, the new single antenna was designed and built. The measured values are similar to the simulated one, measured impedance of the antenna is almost matching with simulated. Simulated radiation pattern is showing the value of gain 1.1dB, which is more than 5dB decrease. That's why no radiation pattern was measured, but only verified by doc. Ing. Jaroslav Lačík, Ph.D., together with reflection coefficients for 50 Ω and 100 Ω . The verified reflection coefficients and radiation pattern are similar with the simulated one.

The first major improvement for the whole antenna design would be a selection of new dielectric substrate. For example, using one of the type of Nylatron or FR4, combined with air slots or making it hollow. Another improvement could be experimenting with different shapes of the patch and adding slots or notches.

Overall, the wrong choice of the dielectric substrate made it difficult to produce the single antenna, which leaded to throwing away the 2-element antenna array production idea. A several ideas were brought to salvage the project but due to lack of time and poor gain of the antenna, only the single antenna was made, measured and verified.

LITERATURE

- [1] Satelitná komunikácia. Satelitná komunikácia [online]. February 2015, 2015, 18 [cit. 2023-11-27]. Available from: <https://vedanadosah.cvtisr.sk/wp-content/uploads/importovane/img/uploads/xzqhzI7P.pdf>
- [2] Advantages and disadvantages of Microstrip Patch Antenna. RF Wireless World [online]. 2013 [cit. 2023-11-27]. Available from: <https://www.rfwireless-world.com/Terminology/Advantages-and-Disadvantages-of-Microstrip-Patch-Antenna.html#:~:text=Drawbacks%20or%20disadvantages%20of%20Microstrip%20Antenna&text=%E2%9E%A8It%20offers%20low%20efficiency,has%20lower%20power%20handling%20capability.>
- [3] Tracking Software - WinListen. DK1TB Website [online]. 2011 [cit. 2023-12-16]. Available from: <http://www.dk1tb.de/indexeng.htm>
- [4] Brno. In: Wikipedia: the free encyclopedia [online]. San Francisco (CA): Wikimedia Foundation, 2001- [cit. 2023-12-17]. Available from: <https://en.wikipedia.org/wiki/Brno>
- [5] Spitsbergen. In: Wikipedia: the free encyclopedia [online]. San Francisco (CA): Wikimedia Foundation, 2001- [cit. 2023-12-17]. Available from: <https://en.wikipedia.org/wiki/Spitsbergen>
- [6] Angle of Elevation. Biju's [online]. 2023 [cit. 2023-12-17]. Available from: <https://byjus.com/maths/angle-of-elevation/#:~:text=The%20angle%20of%20elevation%20is%20an%20angle%20that%20is%20formed,is%20an%20angle%20of%20elevation>
- [7] Azimuths. NWCG [online]. 2013 [cit. 2023-12-18]. Available from: <https://www.nwcg.gov/course/ffm/location/62-azimuths#:~:text=An%20azimuth%20is%20the%20direction,and%200%20degrees%20mark%20north.>
- [8] FR-4. Atlas Fibre [online]. 2023 [cit. 2023-12-19]. Available from: <https://www.atlasfibre.com/material/fr-4/>
- [9] FR4 Dielectric Constant and Material Properties. Altium [online]. 2023 [cit. 2023-12-19]. Available from: <https://resources.altium.com/p/fr4>
- [10] Nylatron. In: Wikipedia: the free encyclopedia [online]. San Francisco (CA): Wikimedia Foundation, 2001- [cit. 2023-12-20]. Available from: <https://en.wikipedia.org/wiki/Nylatron>
- [11] Nylatron. Tribon [online]. 2023 [cit. 2023-12-20]. Available from: <https://www.technicke-plasty-tribon.cz/prodej-plastu/materialy-polotovar/technicke-plasty/nylatron>
- [12] Ertalon® 6 SA PA6. Mitsubishi Chemical Group [online]. 2013 [cit. 2023-12-20]. Available from: <https://www.mcam.com/en/products/shapes/engineering/nylatron-ertalon/ertalon-6-sa-pa6>

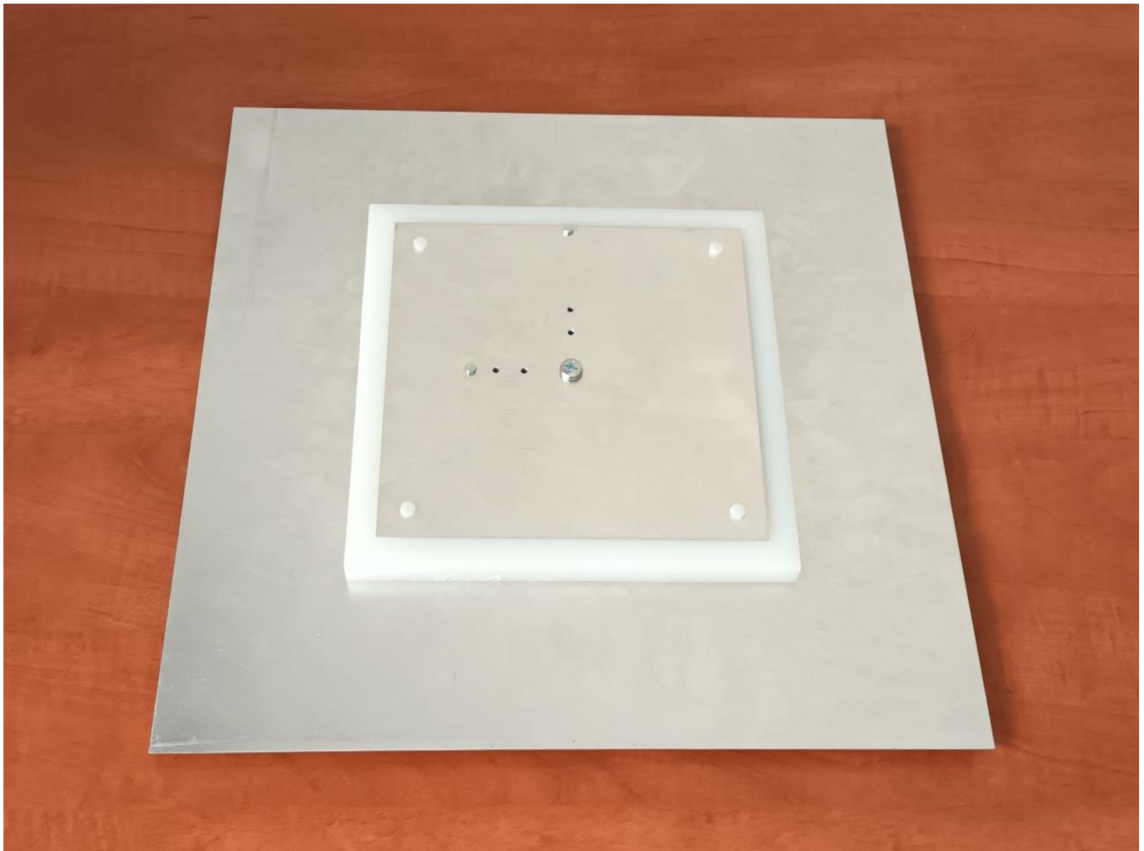
- [13] Ertalon. Tribon [online]. 2023 [cit. 2023-12-20]. Available from: <https://www.technicke-plasty-tribon.cz/prodej-plastu/materialy-polotovarů/technicke-plasty/ertalon>
- [14] *Mikropáskové antény* [online]. 39 [cit. 2023-12-31]. Available from: https://moodle.vut.cz/pluginfile.php/509804/mod_resource/content/1/P3s.pdf
- [15] S-Parameters. *Antenna-Theory.com* [online]. 2015 [cit. 2023-12-26]. Available from: <https://www.antenna-theory.com/definitions/sparameters.php#:~:text=S11%20represents%20how%20much%20power,antenna%20and%20nothing%20is%20radiated.>
- [16] Radiation Pattern. In: *Wikipedia: the free encyclopedia* [online]. San Francisco (CA): Wikimedia Foundation, 2001- [cit. 2023-12-27]. Available from: https://en.wikipedia.org/wiki/Radiation_pattern
- [17] BDSAT-2. *N2YO.com* [online]. 2013 [cit. 2023-12-28]. Available from: <https://www.n2yo.com/satellite/?s=55098>
- [18] *Mutual Coupling*. Online. MathWorks. 2013. Available from : <https://www.mathworks.com/help/antenna/ug/mutual-coupling.html>. [cit. 2024-05-01].
- [19] *A Practical Guide to the Design of Microstrip Antenna Arrays*. Online. Microwavejournal. 2001. Available from: <https://www.microwavejournal.com/articles/3144-a-practical-guide-to-the-designof-microstrip-antenna-arrays>. [cit. 2024-05-01].
- [20] *Flexible RG316 Coax Cable Single Shielded with Tan FEP Jacket Specifications*. Online. Pasternack. 2019. Available from: <https://www.pasternack.com/images/productpdf/rg316-u.pdf>. [cit. 2024-05-01].
- [21] *Činitel zkrácení*. Online. Vf-elektronika-foto. 2017. Available from: https://www.vf-elektronika-foto.cz/K1_files/04.pdf. [cit. 2024-05-01].
- [22] *RF Coaxial Cable Impedance Calculator with Formula*. Online. Pasternack. 2013. Available from: <https://www.citacepro.com/dok/hz1xVURqiLi22gqX>. [cit. 2024-05-03].
- [23] *Antenna Arrays*. Online. RF Elements. April 12th 2022. Available from: [z: https://rfelements.com/blog/antenna-arrays](https://rfelements.com/blog/antenna-arrays). [cit. 2024-05-06].
- [24] *SAT File Format*. Online. Spatial. 2022. Available from: <https://www.spatial.com/resources/glossary/sat-file-type#:~:text=It's%20used%20to%20exchange%203D,%20Daided%20engineering%20C%20and%20more..> [cit. 2024-05-10].

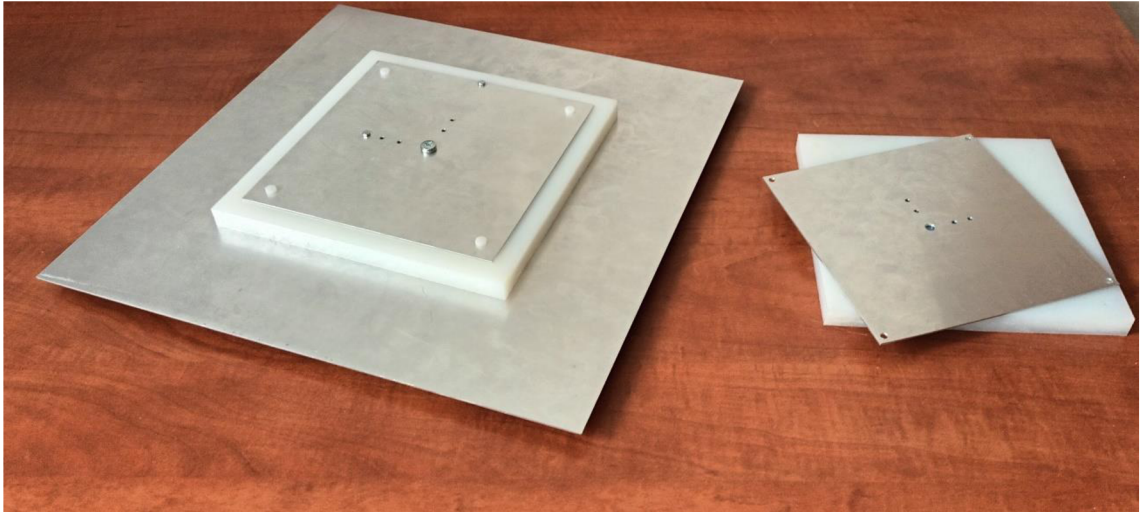
LIST OF APPENDICES

APPENDIX A - PHOTOS OF THE ANTENNA 61

Appendix A - Photos of the antenna

Photos of the single antenna





Photos of the workplace and the antenna during measurement

